FIRAT UNIVERSITY
GRADUATE SCHOOL OF NATURAL AND APPLIED SCIENCES
TÜRKİYE

GREEN SYNTHESIS OF SILVER, COBALT AND SILVER-COBALT BIMETALLIC NANOPARTICLE BY USING P.HARMALA SEED: ANTIMICROBIAL ACTIVITY

Roshna Ashraf ARIF

Master's Thesis

DEPARTMENT OF CHEMISTRY

Division of Analytical Chemistry

JULY 2021

FIRAT UNIVERSITY
GRADUATE SCHOOL OF NATURAL AND APPLIED SCIENCES
TÜRKİYE

Department of Chemistry

Master's Thesis

GREEN SYNTHESIS OF SILVER, COBALT AND SILVER-COBALT BIMETALLIC NANOPARTICLE BY USING P.HARMALA SEED: ANTIMICROBIAL ACTIVITY

Author
Roshna Ashraf ARIF

Supervisor
Prof. Dr. Habibe ÖZMEN

JULY 2021
ELAZIG

FIRAT UNIVERSITY
GRADUATE SCHOOL OF NATURAL AND APPLIED SCIENCES
TÜRKİYE

Department of Chemistry

Master's Thesis

Title:	Green Synthesis of Silver, Cobalt and Silver-Cobalt Bimetallic Nanoparticle by Using P.Harmala Seed: Antimicrobial Activity
Author:	Roshna Ashraf ARIF
Submission Date:	14 June 2021
Defense Date:	08 July 2021

THESIS APPROVAL

This thesis, which was prepared according to the thesis writing rules of the Graduate School of Natural and Applied Sciences, Fırat University, was evaluated by the committee members who have signed the following signatures and was unanimously approved after the defense exam made open to the academic audience.

		Signature
Supervisor:	Prof. Dr. Habibe ÖZMEN Firat University, Faculty of Science	Approved
Chair:	Prof. Dr. Mehmet Yaman Firat University, Faculty of Science	Approved
Member:	Prof. Dr. Fırat AYDIN Dicle University Faculty of Science	Approved

This thesis was approved by the Administrative Board of the Graduate School on

..... / ..... / 20 .....

Signature

Assoc. Dr. Kursat Esat ALYAMAÇ
Director of the Graduate School

DECLARATION

I hereby declare that I wrote this Master's Thesis titled " Green Synthesis of Silver, Cobalt and Silver-Cobalt Bimetallic Nanoparticle by Using P.Harmala Seed: Antimicrobial Activity " in consistent with the thesis writing guide of the Graduate School of Natural and Applied Sciences, Firat University. I also declare that all information in it is correct, that I acted according to scientific ethics in producing and presenting the findings, cited all the references I used, express all institutions or organizations or persons who supported the thesis financially. I have never used the data and information I provide here in order to get a degree in any way.

08 July 2021

Roshna Ashraf ARIF

PREFACE

Before writing the paper "Green Synthesis of Nanoparticles: What Is It?" The basics are to minimize waste and implement sustainable processes. In recent years, the development of nanotechnology to promote environmental sustainability has emphasized a green process using mild reaction conditions and non-toxic precursors. I was engaged in research and writing of this treatise from January to December 2020.

This project was carried out at the request of Prof.Dr. Habibe ÖZMEN. My research question was created with my boss Habibe ÖZMEN. The research was difficult, but conducting extensive investigation has allowed me to answer the identified questions. All subsequent work was carried out at the Institute of Chemistry, Faculty of Science, University of Firat. All project and related methods have been approved by the Graduate School of Applied Sciences, Firat University. PhD student.Şule İNCİ was involved in one stage of concept formation and contributed to antibacterial activity. Habibe ÖZMEN was the director of this project and was involved in concept formation and manuscript creation throughout the project.

I was the Principal Investigator for the projects in Chapters 3 and 4, and responsible for all major areas of concept development, data collection, analysis, and most of the manuscript preparation. Dr. Yakup SAY contributed to data collection and XRD, EDS, and SEM analysis.

Roshna Ashraf ARIF
ELAZIG, 2021

TABLE OF CONTENTS

Page

ABSTRACT

Green Synthesis of Silver, Cobalt and Silver-Cobalt Bimetallic Nanoparticle by Using P.Harmala Seed: Antimicrobial Activity

Roshna Ashraf ARIF

Master's Thesis

FIRAT UNIVERSITY
Graduate School of Natural and Applied Sciences

Department of Chemistry

July 2021, Page: xi + 60

Metallic nanoparticles, it has very unique property, due to its improved its size, distribution and morphology, the synthesis of nanoparticles is increasing among researchers and their manufacture and widespread use in many scientific fields has begun. For example, it has applications in a variety of fields, including drug delivery, optoelectronics, optical, magnetic, thermal, electrical devices, sensors and cosmetics.

In this study we synthesized silver nanoparticle (Ag NP), cobalt nanoparticle (CoNP) and silver-cobalt nanoparticle (Ag-CoNP), using Peganum harmala seed, extracted in three different solvent, water, methanol and ethanol, at ambient temperature. The synthesized nanoparticles NPs were characterized using UV–Vis spectrophotometer, X-ray diffractometer (XRD), Fourier transforms infrared spectroscopy (FT–IR), energy dispersive X-ray spectroscopy (EDS) and scanning electron microscope (SEM).

Inhibitory activity was performed for the three of the synthesized nanoparticles NPs was performed by well diffusion method against human pathogens like Escherichia coli, Staphylococcus aureus and Candida albicans. The highest antimicrobial activity of silver nanoparticles synthesized by methanol of Peganum harmala seed extracts was found against S. aureus (16 mm) and C. albicans (16 mm) respectively. The nanoparticles NPs synthesized in this process have the efficient antimicrobial activity against pathogenic bacteria

Keywords: Silver Nanoparticles, Cobalt Nanoparticle, Ag-Co Bimetallic Nanoparticle, Antimicrobial Activity, Green Synthesis, Peganum harmala

ÖZET

P. Harmala Tohumu Kullanılarak Gümüş, Cobalt ve Gümüş- Kobalt Bimetalik Nanopartüküllerinin Yeşil Sentezi. Antimikrobiyal Aktiviteleri

Roshna Ashraf ARIF

Yüksek Lisans Tezi

FIRAT ÜNİVERSİTESİ
Fen Bilimleri Enstitüsü

Kimya Anabilim Dalı

Temmuz 2021, Sayfa: xi + 60

Metalik nanopartiküller, çok özel bir özelliğe sahiptir, Nanopartiküllerin büyüklüğü, dağılımı ve morfolojisini geliştirmesi nedeniyle araştırmacılar arasında sentezi artmakta ve bunların üretimi ve birçok bilimsel alanda yaygın olarak kullanılmaya başlanmıştır. Örneğin, ilaç dağıtımı, optoelektronik, optik, manyetik, termal, elektrikli cihazlar, sensörler ve kozmetikler dahil olmak üzere çeşitli alanlarda uygulamaları vardır. [32], [33].

Bu çalışmada Peganum harmala tohumu, üç farklı çözücü kullanılarak, su, metanol ve etanol içinde ekstrakte edilmiş ve bu ekstraklar kullanılarak gümüş (AgNP), kobalt (CoNP) ve gümüş-kobalt (Ag-CoNP) nanopartikülleri oda sıcaklığında sentezlendi. Sentezlenen nanopartiküllerin, UV-vis spektrofotometre, X-ışını difraktometresi (XRD), Fourier dönüşümü kızılötesi spektroskopisi (FT-IR), enerji dağıtıcı X-ışını spektroskopisi (EDS) ve taramalı elektron mikroskobu (SEM) kullanılarak karakterize edildi.

Sentezlenen nanopartiküller; Escherichia coli, Staphylococcus aureus ve Candida albicans gibi insan patojenlerine karşı inhibe edici aktivite değerleri belirlendi. Peganum harmala tohumunun metanol ekstraktları ile sentezlenen gümüş nanopartiküllerin en yüksek antimikrobiyal aktivitesi sırasıyla S. aureus (16 mm) ve C. albicans (16 mm) 'ye karşı bulundu. Sentezlenen bütün nanopartiküller, patojenik bakterilere karşı etkili antimikrobiyal aktiviteye sahiptir

Anahtar Kelimeler: Gümüş Nanopartiküller, Kobalt Nanopartikül, Ag-Co Bimetalik Nanopartikül, Antimikrobiyal Aktivite, Yeşil Sentez, Peganum harmala

LIST OF FIGURES

Page

LIST OF TABLES

Page

SYMBOLS AND ABBREVIATIONS

Symbols

Hrs : Hours
nm : Nanometer

Abbreviations

AgNPs	: Silver nanoparticles
Ag-CoNPs	: Silver-cobalt nanoparticles
CoNPs	: Cobalt nanoparticles
FTIR	: Fourier Transmission Infra-red
NPs	: Nanoparticles
SEM	: Scanning Electron Microscopy
UV-Vis	: Ultraviolet-Visible
XRD	: X-Ray Diffraction
WE	: Water extract
EE	: Ethanol extract
ME	: Methanol extract

1. INTRODUCTION

Nanotechnology is a rapidly growing field that is gaining great interest from researchers, and it has entered various research fields, which is a scientific field that deals with nanometric materials or structures, usually in the range of 1-100 nanometers. It is a science that deals with monocular Nano-objects, materials, and devices based on them, and processes that take place in the nanometer range, giving a variety of focus to diverse disciplines of science such as dentistry, pharmaceuticals, and bioengineering.[1-2].

Nanomaterial with characteristic dimensions in the range of 1-100 nm is at the forefront of Nanoscience and nanotechnology. Due to the tiny size of the nanoparticles and the high ratio of surface area, the physical and chemical properties of the material containing the nanoparticles are completely different from the physicochemical properties of the bulk material. Nanomaterials, especially metallic nanoparticles, have gained a keen interest in applied sciences in various fields from materials science to biotechnology in recent years [3].

The widespread practical application of metal nanoparticles is due to a number of their unique properties [4]. Today, a variety of physical and chemical processes are widely used in the synthesis of metal nanoparticles, which can result in particles with the desired properties [5]. Due to the high demand for the manufacture of nanomaterials, the development of a wide range of industrial methods for synthesizing metal nanoparticles has been developed [6]. However, it is necessary to use clean, free of toxic and environmentally friendly methods to synthesize nanomaterials, [7] because some methods use toxic solvents and high energy, which in turn are harmful to the environment and living organisms [5]. Due to efforts to rehabilitate the environment, synthetic methods have been found that incorporate environmentally friendly protocols. Green synthesis methods are increasingly recognized in the fields of chemistry and chemical technology. They offset the high manufacturing costs and high energies associated with the accustomed methods of synthesizing nanoparticles through conventional techniques that use dangerous chemicals such as sodium borohydride and hydrazine [7].

With the use of natural sources and ideal solvent systems (such as bio-organic systems) for, reduction NPs has a significant impact on the morphology of incorporated particles, such as the size, physicochemical properties, shape, and NPs utilization. The natural source that has been adopted in the manufacture of mineral nanoparticles is called green synthesis, in which diverse biological materials such as (bacteria, plant extracts, fungi, algae, and, etc.) are used. [1] It was found that the plant extracts are fairly unpretentious for large-scale production of nanoparticles compared to bacterial and fungal synthesis methods. It is a simple process, among the green synthesis methods. Which are known collectively as biogenic particles [8].

Plants or plant extracts for the synthesis of metals and metal hybrid nanoparticles have now become the focus of widely accepted new research [7]. In addition, the ability to adjust the physical and chemical properties of nanomaterial's or noble metal nanoparticles, therefore, they have found relevance in the fields of electronics, photochemistry, biomedicine, chemistry, catalysis, and photonics. This can be the result of small size with large specific surface area, quantum size effect, and electronic structure. [9-10]

Before using the green synthesis method to synthesize nanoparticles, the Creighton method was used to synthesize silver nanoparticles (AgNPs) for a long period of time, by using sodium borohydride (NaBH4) as the reduction of silver nitrate. This procedure often yields 10 nm. Which was also used for synthesizing other metals such as Pt, Ni, Cu, and Pd [11]. Also, the first use of plant extracts was selected from endemic or global biological differences. It was found that using extracts from different parts of plants and their seeds in the presence of mineral salts leads to the production of nanoparticles of different sizes, shapes, formulations, and activities [12].

Many studies on the green synthesize of metal NPs studies the reduction of precious metals such as gold (Au), silver (Ag), and platinum (Pt), and other minerals such as copper (Cu) [12] Those precious metal nanoparticles are of particular importance due to their unique size and shape-dependent photoelectric properties, of which silver is among the three metals (Ag, Au, Cu). It is found that it has the highest efficiency. Plasmon's resonance appears in an adjustable wavelength in the visible spectrum [7-13].

In this study, we used Peganum Harmala seeds for the green synthesis of Ag, Co, and Ag-CoNPs. The reason for using Harmala P seeds for their pharmacological effects was used as an important medicinal plant in folk remedies around the world and is said to be used to treat various conditions such as low back pain. Traditional reproduction of P. Harmala is from seeds and has some restrictions, including germination. Seeds smoke has been used by Iranians as a disinfectant and disinfectant approach, but at high doses, it is toxic and can cause paralysis. It is applied as traditional medicine for its long-term antibacterial, fungicide, and herbicide effects [14].

P. Harmala contains a variety of alkaloids, which are β-carboline and quinazoline alkaloids that are difficult to synthesize. Those to the structure are responsible for the toxicological and pharmacological effects of plants. However, extracts from its ripe fruits and flowers contain structurally simple compounds. [14] β-Carbolin alkaloids are abundant in many plant families and have neurostimulator and monoamine oxidase (MAO) inhibiting activity, which have drawn the attention of scientists to their severe inhibitory effects on certain antibiotic-resistant strains [15-16].

Many studies have synthesized silver nanoparticles and copper nanoparticles, and a few of them have studied the manufacture of bimetallic silver-copper nanoparticles. For the first time in this research, we tried to synthesize silver-copper nanoparticles and copper nanoparticles, using

Haramala seeds, and this is due to the importance of each of the three products of the aforementioned, whether, from medical or industrial point fields, researchers are especially interested in the synthesizing of silver and copper.

Among the many nanomaterials, silver has gained increasing interest in various fields, especially in marketing. Due to its special high surface area, unique physical and chemical properties, some of these fields, including conductivity, chemical stability, Catalytic and antibacterial activity. AgNPs are widely used in health manufacture, as antibacterial agents, food manufacture, food storage, diagnostics, orthopedics, drug acknowledgment, antiseptic agent, and web coating, including anti-angiogenesis and anti-cancer agents [17].

To meet the requirements of AgNPs in general, various synthesis methods have been adopted; the traditional physical and chemical methods are expensive and dangerous. Interestingly, the biologically prepared Ag NPs, called the green approach, showed high yield, solubility, and high stability, and they are simple, fast, non-toxic, and reliable that can produce well-defined sizes and shapes [18].

Also, Co has long been of interest to researchers in a wide range of fields. In general, participating CoNPs have scientific and technological in various fields, such as magnetic composites magnetic sensors, recording media, magnetic fluids, magnetic memories, and catalysis, and the most significant, benefits in areas related to bio-medicine, such as drug delivery and magnetic resonance imaging, all this, thanks to their distinctive properties, of catalytic, magnetic, and electrical, where to avoid alter their magnetization or response stability demand high quality and purity for all these applications [19]. Cobalt nanoparticles (CoNPs) exhibit numerous properties due to their large surface area [20].

Cobalt nanoparticles (CoNP) are highly resistant to oxidation, corrosion, and wear [21]. However, the synthesis of cobalt nanoparticles is very sensitive because many parameters affect their physical and electrochemical properties. Instead of its sensitivity, there are various methods for synthesizing CoNP, but biological methods such as microbial synthesis of nanoparticles. Especially through plants, is becoming more important due to its simplicity, appearance, and environmental friendliness [22].

Thus, the present study was designed for the green synthesis of cobalt nanoparticles in which plant extract Paganum Hermala seed, was used and to detect antimicrobial activity (gram-positive and gram-negative), and the property of nanoparticles.

For the first time in this study, bimetallic Ag-CoNPs were synthesized using green extract of P. Harmala seeds. Binary nanoparticles are formed by combining metallic salt solutions in the presence of a reducing agent, to show new properties due to the simultaneity of the two metals with many structures [23]. Bimetallic nanoparticles have distinct mixing patterns and geometric structures that enhance their functions. They have better stability, selective activity than

monomeric nanoparticles, and they exhibit catalytic activity. Catalysts can also make some chemical changes that were not common with single-metal nanoparticles as catalysts. This is because bimetallic nanoparticles contain a special mixture of two metals, each of which performs a specific function to perform the combinational reaction mechanism. Simply by modifying the individual components as well as the architecture, the physical and chemical properties of bimetallic nanoparticles can be modified for better performance. Bimetallic nanoparticles excluded single-scale nanoparticles due to the better electronic, optical, and catalytic performance [24].

Various studies have shown that Co is used as a core material in Nano composite materials, which including core-shell structures, such as cobalt-gold, cobalt-copper, cobalt-platinum, and cobalt-silver nanoparticles. The advantage of using Co as a base material is providing a giant magneto resistance (GMR) and high stability at high temperatures, temperatures, allowing nanoparticles for multifunctional sensing, media recording, and wideband photovoltaic solar cell applications [25].

Additionally, many natural resources are available for the environmentally friendly formulation of nanoparticles such as plants, plant products, bacteria, fungi, algae, yeast, and viruses. Interestingly, biological molecules can act as reducing agents and blocking agents for nanoparticle synthesis. The blocking agent is essential to prevent the accumulation of nanoparticles and increase the solubility of the nanostructured system, and it can also be used as a bio-binding site for important particles and nanoparticles [26].

1.1. Justification and Problem from research

Evidence of the rapid development of technology is products such as nanoparticles and nanomaterials [27]. Due to its unique properties, it is applied in many fields such as catalysts, cosmetics, electronics, renewable energy, biomedical materials science, physics, environmental improvement, and biology. Regrettably, the utilize of poisonous organic solvents and strong reducing agents to produce nanoparticles creates hazardous wastes that pose a major threat to the environment. [28-29]. Since the demand for nanoparticles is increasing in the field of technology, plant-mediated green synthesis offers an expense-efficacious, easy stage as an extra environmentally friendly and sustainable method [30].

The Nucleation in green synthesis is rapid, unlike the chemical method whose takes 2 hrs. [31]. This technology provides a stable dispersion of nanoparticles that resists agglomeration and is highly resistant to oxidation in biological media, which is of high importance [32].In addition, by using plants and micro-organisms, it is possible to overcome the problems that are directed by chemical methods of using, high energy and wasted purification, to the synthesis of nanoparticles that require purification due to the traces poisonous left on the superficies of the nanomaterials. It has also been suggested that the use of green synthesis cancels out the complex synthesis process [33]. Additionally, this work aims to utilize locally available biomaterials for silver, cobalt, and bimetallic silver-cobalt nanostructures. This is because it lays the foundation for checking the active components of our bio resource to create amount-added products.

1.2. The Purpose of This Research

There is a set of objectives in this research, which includes the synthesis of Ag nanoparticles, Co nanoparticles, and bimetallic nanoparticles Ag-Co using Peganum Harmala seeds, which are as follows:

i. Using a based eco-friendly plant extract as a reducing agent/capping agent to synthesize silver, cobalt, and bimetallic nanoparticles, which most likely will displace the more high-cost chemicals earlier used.
ii. Using a UV-Vis Spectrophotometer, to determine the extent to which the use of various solvents as an extract affects the characterization of silver nanoparticles, cobalt nanoparticles, and silver bimetallic nanoparticles.
iii. To study the properties of nanoparticles using XRD, EDX, and FTIR. To add more particle properties, study the structural engineering properties of particles using SEM.
iv. Study synthesized nanoparticles composition property by using the same plant.

v. Analyze the antimicrobial properties against specific bacteria and fungi, of synthesized nanoparticles.

1.3. Research queries

i. Can the replacement of hazardous chemicals available plant extract act as a reducing and capping agent, for the synthesis of nanoparticles?
ii. For what objective can Green synthetic nanoparticles work?
iii. Can diseases that have caused public health be addressed, through the green synthesis of nanoparticles, a health issue related to abstaining from taking drugs?
iv. Can the plant extract by methanol and ethanol produce nanoparticles as plant extract with water does?

1.4. Theories

The hypothetical concepts of this study are:

i. If chemicals components act as reducing agents then plants wealthy in phytochemicals could be utilized like biodegradable agents.
ii. If chemically produced nanoparticles have antibacterial activity, then green synthetic nanoparticles should serve the same purpose as chemicals product does.

2. LITERATURE REVIEW

2.1. Methods of nanoparticle synthesis

Two processes bottom-up and top-down are the main processes utilize for nanoparticle synthesis, Away from naturally in progress nanomaterials. This approach was suggested by Feynman in 1960 during his lecture at the American Society named (American Physical Society), where the light shone on a point in which he said atomic specifications can adapt to different devices and materials [34]. Of course, his proposal went beyond the wildest imaginations of our time [7].

In general, physical and chemical methods are one of the methods for synthesizing nanomaterials. Chemical methods for the synthesis of nanoparticles are toxic, as the surface of the gross result is absorbed by chemicals and are often mixed in their composition, and this makes the nanomaterials created in this way harmful to their biomedical applications, and this problem can be overcome by using biological methods for the synthesis of nanomaterials, which are known as The synthesis of green nanoparticles can be primarily synthesized using physical and chemical methods [35]. Therefore, this study supplies an overview of the Harmala seeds of green synthesis used in the synthesis of nanoparticles [6].

2.1.1. Top-Down Approach

This approach is to collapse the aggregate material into nano-sized structures or particles. The top-down approach is inherently simpler and produces the desired structure with appropriate properties depending on the elimination or splitting of the bulk manufacturing process. Initially, it involves synthesizing enlarged styles and then their size is minified by deforming the plastic into small nano-sized sizes. Due to its time-consuming and high cost, this technique is not utilized for synthesizing nanoparticles on large scale [36]. This top-down approach has the major problem of imperfections on its surface structure. Examples of these technologies include elevation-energy moisten ball milling, nuclear operation, electron beam lithography, dust spraying, and gas-phase condensation [37].

2.1.2. Bottom-Up Approach

This method involves minifying substance ingredients, down to the atomic size with an additional nanostructure formation that occurs during self-combination operation, in which the physical forces which work on the Nano scale are utilized to bind the essential oneness into a bigger stable structure. Ideal samples are the Organometallic pathway, consider micelle pathway, sol-gel manufacture, colloidal precipitation, hydrothermal synthesis, model-supported sol-gel;

electro deposition, etc., the fabrication of brilliant nanoparticles is a famous technique of bottom-up. An alternative that is likely to be more economical while reducing waste is 'bottom-up' [38].

2.2. Green Synthesis

Green synthesis is currently the focus of new research among the various technologies for synthesizing nanoparticles. due to the elevation of the cost and hazards of methods such as physical and chemical, The green synthesis pathway becomes more desirable to produce nanoparticles, and this method has been accepted cause to its environmentally eco-friendly [39]. Green synthesis utilizes a bottom-up approach method, involving either a reduction reaction or an oxidation reaction. Green synthesis pathways include, the utilize of microscopic organisms such as bacteria, yeasts, fungi, algae, and viruses), and plant parts, or plant extracts [40-41].

2.2.1. Microorganisms Used to Synthesis Nanoparticles

Bacteria, fungi, actinomycetes, moss, and leaven, are microorganisms that have been utilized for the biosynthesis of a wide range of nanoparticles in both extracellular and intracellular, such as gold, iron, lead, cadmium, and most used nanoparticle silver [42-43]. Extracellular biosynthesis of nanoparticles has been extensively studied it eliminate the downstream processing steps required for nanoparticle recovery [44]. Singh et al [43] discovered that microbial enzymes, peptides, reducing cofactors, and organic materials play important roles in bioreduction to produce nanoparticles. In addition, the report by Mukherjee, P., et al. [45] clarifies that the reduction of metal ions could be occurred by the cell walls and their proteins.

Siavash Iravani reported that [46] bacteria nominee as the preferable microorganism for the synthesis of nanoparticles, due to having the salient capability to reduce heavy metal ions. Klaus, Joerger, Olsson & Granqvist, 1999 [47] developed silver and gold nanoparticles using prokaryotes such as Pseudomonasstutzeri AG259 and Proteus mirabilis PTCC 1710 cultured in high concentrations of AgNO3. [48] According to a study carried out by Mullen et al. [49] on different types of bacteria, such as Bacillus cereus, Bacillus subtilis, E. coli, and Pseudomonas aeruginosa they showed the ability to reduce ions of silver, cadmium, copper, and lanthanum. Saifuddin et al. [50], Kalishwaralal et al. [51], and Nair, B., & Pradeep, T. [52] have characterized approach method for green biosynthesis of silver NPs. by using (Bacillus subtilis, Bacillus licheniformis, and Lactobacillus Strains) respectively.

Ahmad et al., [53] first described fungal-mediated green nanoparticle synthesis using Desmodium triflorum. This had advantages over the intracellular method over non-binding to biomass (Duran, Marcato, Alves, de Souza & Esposito, [54]; Balaji et al., [55]; Ahmad et al., [53]). The study, making silver nanoparticles, from outside the cell using the green yeast method. Also, (Mandal et al., [56]; Mourato, Gadanho, Lino & Tenreiro, [57]; Apte, Sambre & Gaikawad,

[58]). They succeeded in creating gold nanoparticles, using algae (eukaryotic autotrophs). A 2007 study revealed that highly stable nanoparticles can be synthesized using Sargassumwightii seaweed in a study by Singaravelu [59] The properties of nanoparticles synthesized via algae have been more stable than other green routes. Table 2.1is an edited table showing some metal nanoparticles synthesized by microorganisms.

Table 2.1: Study of utilize some microorganisms in synthesis of Metal nanoparticles

Type	Nanoparticles	Diameter (nm)	Reference
Bacillus Subtilis	Ag	5-50	[50]
Bacillus licheniformis	Ag	10 - 15	[51]
Lactobacillus Strains	Ag	15-100	[52]
Pseudomonas stutzeri AG259	Ag	200	[47]
Proteus mirabilis PTCC 1710	Au	10 - 20	[48]
Desmodium triflorum	Ag	5-20	[53]
Psychrotrophic yeast Yarrowia lipolytica NCYC 789	Ag	Not available	[58]
Cladosporium cladosporioides fungus	Ag	10-100	[55]
Fusarium oxysporum strains	Ag	20 -50	[54]
Extremophilic Yeasts	Ag-Au	30-100	[57]
marine alga, Sargassum wightii Greville	Au	8 , 12	[59]

2.2.2. Green Synthesis plant extract of Nanoparticles

Biodiversity exploration using plants or plant extracts as the production assembly of nanoparticles is drawing attention due to its rapid, environmentally friendly, non-pathogenic, and economical protocols, and can be easily Nanoparticle synthesis, in the high range of scale [60]. In general, plant extract-mediated reduction is simply mixing the extract with an aqueous metal precursor at room temperature or a certain fixed temperature. Metabolites commonly present in plant extracts such as terpenoids and phenols, Proteins, or carbohydrates, contain active functional groups such as aldehydes, amines, and carboxyl substances which much literature had reported the presence of phytochemicals in many plants. Those active functional groups are considered a source of reducing, stabilizing, and capping agents for NP synthesis [61]. Thus, in contrast to chemical methods of nanoparticle synthesis, which use harsh and highly poisonous chemicals that are overwhelmingly adsorbed to the surface of nanoparticles, the synthesized nanoparticles are not suitable for medical use [62]. Each extract contains various concentrations and combinations of reducing and stabilizing agents, that determines the properties of the synthesized

NP. Some plants that promote metallic nanoparticle synthesis have been reported and mentioned in (Table 2.2) and briefly discussed in the below review [60].

Table 2.2: Nanoparticles synthesized by different researchers Plant extracts.

Plants and parts of the plant used	Nanoparticles	Diameter (nm)	Reference
Amaranthus gangeticus Linn leaf	Ag	11-15	[63]
Peganum harmala seed	ZnO	40	[64]
Euphorbia heterophylla L. leaves	Co_3O_4	69.75	[66]
Canna indica leaf	Ag Ag/Ni	9.10-+1.12 9.86-+2.37	[67]
Geranium route	Ag	15-50	[68]
Cannabis sativa leaf	Ag, Au, Ag-Au	Not available	[72]
Camellia sinensis (L.) Kuntze and Apium graveolens L.	Co_3O_4	21-55	[73]
Ocimum Sanctum (Tulsi) leaf	Ag	10-20	[69]
Ocimum tenuiflorum Solanum tricobatum Syzygium cumini Centella asiatica Citrus sinensis	Ag	28 22.3 26.5 28.4 65	[70]
Glycyrrhiza glabra Amphipterygium adstringens	Ag	1-10	[71]
Passiflora foetida.leaves	Cu	150-300	[74]

Kolya, et al [63] fabricated silver nanoparticles. By utilized of Amaranthus gangeticus Linn leaf. In this experiment, the reaction was the conceivable cause of the presence of amino acids in the leaf extract which responsible for reducing the silver ion to silver nanoparticles in the nanoscale.

Peganum Harmala seed extracts used by some researcher, for synthesizing different nanoparticles, such as ZnO nanoparticles, in this work, Fazlzadeh, et al [64] coated the activated carbon powder where derived from Peganum Harmala seed (PPAC), by green zinc oxide nanoparticles for removal application of Chromium (VI). The same plant was used by Matin Azizi et al [65] out with the utilize water extracted of Peganum Harmala for the synthesis of silver nanoparticles at surrounded room temperature, with an average particle size of 23 nm.

Mulya Dewi, et al [66] the green synthesis of cobalt oxide nanoparticles was reported by utilized Euphorbia heterophylla L. leaves, in this study, the cobalt oxide nanoparticles had spherically shaped with the particle size of about 17 nm. Many researchers synthesize Ag nanoparticles by using different plant extract. Each AgNPs shows various characterize and antimicrobial activity. This is because the concentration and combination of compounds such as phenols, alkaloids, and flavonoids are different depending on the extract, and the reduction process is relatively complex [67-71]. As reported by Abbasi et al. [72], they synthesized gold

and silver bimetallic nanoparticles, compared to the same particles alone from both silver and gold, which showed improvement in microbial activity against Bacillus subtilis and Pseudomonas aeruginosa. The results indicate that bionic nanoparticles can be used as powerful antibiotics, while another investigator could look at the formation of both nanoparticles and bimetals using organic materials rich in phytochemicals instead of environmentally harmful organic materials.

Aliya A. Urabe and Wisam J. Aziz [73] both worked on synthesizing cobalt-oxide nanoparticles by using two different plants extract as reducing agent. They reported that the best achievable result in inhibiting bacteria comes by using Camellia sciences extract by (27-29 mm), rather than Apium graveolens extract. Akineseko, A., et al, and others. They revealed different shapes of Ni-Silver binary nanoparticles: the cube-shaped with average size, cut edges and irregular particle size was 9.86 ± 2.37 nm as confirmed by TEM. The spectrum of the EDX analysis also showed the elemental structures of the nanoparticles which indicated that the nanohybrid was enriched with the organic dam due to the formation of the carbon content that originated from the plant extract. Based on this report, due to the observation of the inhibitory strength of bimetallic nickel and silver nanoparticles, it is possible to design antibacterial drugs [67].

Subha et al. [74] worked on the synthesis of copper nanoparticles medium size of copper nanoparticles (24.54 nm). According to this study, the copper nanoparticle-drug-gelatin complex controls atorvastatin calcium release better than ATC-gelatin film, thus combining the advantages of the gelatin film and Cu NPs-ATC interactions to provide better-sustained release performance. Just a few examples of green synthesis of nanoparticles, researchers today are still using plant-mediated green synthesis to develop nanoparticles and nanomaterials [7].

2.3. **Microorganisms Pathogenicity**

Microorganisms that can cause ailment in plants, animals, or mealybugs are known as pathogens, biological factors that can damage the steward during the interaction. It can affect people or animals directly or indirectly. Damage to the host can be caused by toxic or toxic factors. The initial harm is caused directly by the organism, while the second direct harm is due to the host immune response activity. The pathogenesis can be described as the ability of a microorganism to transport ailment or to convert a host organism into a disease [75]. The disease that causes the pathogens can be opportunistic, compulsory, or facultative. Pathogens that require a living host for reproduction and survival are obligatory. Notwithstanding can affect the sanitary immune system of sensitive host species for example, of susceptible host types. Mycobacterium tuberculosis [76]. Opportunistic pathogens are less malignant to healthy hosts. And thrive on organic substrates. They attack the host with the possibility of a powerful and slow compromised immune response [77]. The reaction between the hosts and the pathogens affects the Key-and-

lock method. The support of the genetic structure of both hosts and pathogens is provided through Molecular interaction.

Genetic variations, selection of the best mutants, and maintenance (or progression into disease) are key processes for altering the interaction [78]. Many pathogens attach themselves to their hosts by sticking to microorganisms [79]. Germinal variation, chosen of the best mutants, and maintenance (or advancement into ailment) are key operations for altering the interaction [78]. Many pathogens attach themselves to their hosts by sticking to microorganisms [79]. But it either enters the body or infiltrates the host. Just as Salmonella, Mycobacterium spp., Shigella, and Chlamydia it causes intracellular infection, or extracellular as occurred in Pseudomonas aeruginosa. Pathogens occur, because of the surface-exposed proteins, intracellular bacterial diseases can be introduced into the host cell through an active invasion process [80]. Pathogenic bacteria in plants called extracellular are fundamentally microorganisms that enter host tissues through injuries or natural holes in the leaf and geminate in, such as stomata and microscopic holes. Fungal pathogens of most mammals are also thought to be extracellular, with some hosts attacking the cytoplast [81].

2.3.1. Pathogenicity of Staphylococcus Aureus

S. aureus cells known as a smooth surface with ball-shaped gram-positive. When they are observed under a microscope after a gram stain, they are often in clusters of grapes [82]. Diameter from 0.5 to 1.0 μM. The name 'Staphylococcus' comes from the Greek language, which means grapefruit (staple) and berry (Kokko) [83]. It is an effective human pathogen. It is a widespread contagion of healthy skin, leather glands, and mucoid diaphragms. According to GOULD, D., et al [84] 30% of the general population have S. aureus in normal skin flora.

S. aureus is an anaerobic and elective anaerobic creature that which produce settlement of considerable size with yellow or white color on the nutrient-rich agar media, producing energy through aerobic inhalation and fermentation resulting in lactic acid [85]. The organism is often hemolytic in the blood, because of the manufacture of four species of hemolysis (alpha, beta, gamma, and delta), [86]. Almost all of the isolated S. aureus produces coagulase enzymes, a virulence element that also helps identify organisms [87]. Lindsay, J. A., et al. [88] found that it is still a common cause of hospital-acquired infections and is often the cause of wound infections after surgery. As noted, each year, approximately 500,000 patients in the United States hospital receive staphylococcal infections, S. aureus [89].

DieKema and his colleagues found out about injuries that occur in the lower respiratory tract, blood flow, skin, and smooth tissue infections through S. aureus. It has also been found that pathogens develop antimicrobial resistance apart from other serious infections resulting from them [90]. Many common virulence agents are responcible of the degree of the pathogenesis of S. aureus (virulence operator) [91]. This includes, moreover, endocytic infections caused by secret

manufactures like "α, β, γ-hemolysin, leukocidin and Panton-Valentine leukocidin (PVL)" that cause and also cause osmotic cell lysis [92], adhesion operators: are caused colonization which related to cellular peptidoglycans, by many covalent bonds [93].

2.3.2. Pathogenicity of Escherichia Coli

Escherichia coli are a gram-negative bacterium that inhabits the large intestine in humans and makes up about 80% of its aerobic flora. Note that anaerobe germs predominate in its intestine. This bacterium may be non-pathogenic in its basic medicinal effects, and it is a source of vitamin K, but many of its strains cause different types of intestinal, urinary, and other infections. It may cause diseases such as internal bleeding due to Escherichia coli [94]. It has various virulence factors such as toxins and enzymes. It also ferments a wide range of carbohydrates and most of its individuals are fermented for lactose. It is also negative for the oxidase test. It is positive for the catalase test. It has the ability to reduce nitrate to nitrite for the purpose of producing energy. Flagella, not forming spores and the optimum temperature for their growth (37) are one of the most important members of the intestinal family and grow like a normal flora in the digestive system [95]. It is also a pathogen opportunistic bacterium, which causes diarrheal diseases called Diarrheagenic E.coli (DEC) as well as many diseases outside its habitats natural including meningitis neonatal and sepsis [96]. Escherichia coli is one of the sensitive bacteria, as it has the ability to change the diameter of its outer pore membrane to obtain nutrients, prevent inhibitors, and all this happens once the pH and temperature change. An example of temperature, he can also sense the presence of chemicals to which he responds by moving away from them. The presence of Escherichia coli in the human intestine and ducts is an analytical tool for the detection of water and gastrointestinal contamination. Therefore, wherever Escherichia coli is found, it can be contaminated with human infectious parasites [97].

2.3.3. Pathogenicity of Candida Albicans

Candida albicans is an opportunistic mold that attack persons with weak inviolability, and also the healthy people. Has been discovered to be a harmless if the ratio was about 70% lives with symbiosis in the genitourinary and gastrointestinal tract. Researchers have shown that 3 out of 4 women are preys of this microbial contagion once in their lifetime [98-99]. C. Albicans, it is a reason of renowned pathogenic which known as Candidiasis. It is also because mucosal infections, it can range from thrush to the gastrointestinal epithelial cells, vaginal, or pharyngeal mucosa. It causes two widespread infections in woman, which are, frequent Volvo Vaginal Candidiasis (FVVC) with a Volvo Vaginal Candidiasis (VVC) it is common in women. Contagion can be existence-menacing in people with HIV, faint weight in newborn, and those with chemotherapy [100-101]. The C. albicans is considered as extremely contagious molds

distinct to other non-albicans genus Candida glabrata such as, Candida parapsilosis, Candida dubliniensis, Candida krusei, and Candida tropicalis [102] discovered from alternative humans. Mortality elevated about 50% through via bloodstream infection in C. Albicans contagion [103]. The figuration of biofilms produces high grades of drug reluctance to abundant antifungal drugs [104]; dislocated cells the biofilms widely resistant to obtainable medicines than free-living plankton [105].

2.4. **Description and medicinal properties of P. Harmala**

Harmal (Peganum harmala) Medicinal plants of the family Zygophyllaceae, with versatility, because of the similarity to plants of the family of rue, called Syrian rue or wild rue. It is a long-lived plant, usually up to 0.3 m in length, if suitable soil can reach 0.8 m in length, and the depth of its root able to go up to 6.1 meters if the soil is dry. It blooms in the northern hemisphere between June and August. It is an herb with whitish flowers, as showed in (Figure 2.1) Its seeds are round in shape, divided into three tents, each tent containing more than 50 seeds with a diameter of 1-1.5 cm, and the diameter of its flower is about 2.5-3.8 cm. [106] It is known in folk medicine for its use as an antiseptic and a pain reliever. It was also used to treat many diseases such as asthma, back pain, colic, and as a menstrual tonic [107]. The seeds possessed hypothermic and primarily hallucinogenic properties [108].

This species has a number of therapeutic purposes that primarily emphasize neuropharmacology, antidepressant, and hallucinogenic activity. This activity comes from β-carboline, and its seeds are common with the β-carboline [109]. Through several studies of different parts of the plant from seeds, roots, flowers, and stems, for their antimicrobial activity, each part was evaluated and compared, and the result showed that the extracts of seeds and roots have the best activity against gram-positive and gram-negative. Gram-positive bacteria such as Staphylococcus aureus, L. monocytogenes, B. anthracis, Staphylococcus epidermidis, B. cereus, Streptococcus pyogenes, and Bacillus pumilusand, and Gram-negative bacterial type are Proteus mirabilis, E. coli, Klebsiella pneumonia, B. melitensis, Salmonella typhi, and P. aeruginosa [110]. Chemical components in the P.harmala are alkaloids, flavonoids, and anthraquinones which known as known phytochemical components [111].

(a) **(b)**

Figure 2.1: Peganum Harmala plant, a) Dry seed, b) Flower [112]

3. MATERIALS AND METHODS

3.1. Reagents and Equipment

The reagents that we used: Was Silver nitrate ($AgNO_3$), and Cobalt Nitrate hexahydrate ($Co(NO_3)_2.6H_2O$). Qualitative filter paper 125 mm, watch glasses, measuring cylinders, different sizes of tube, pipet, volumetric flasks clear glass, mortar pestle glass, beakers, distilled- deionized water, methanol, ethanol, Dry Food Grinder Machine, Coffee Bean Grinder, Magnetic Stirrer. Internal digital (Shimadzu Corporation, Japan) analytical balance with a readability of 0.01 mg, used during the experiment.

3.2. Equipment

The following equipment was used: The infrared spectrum is registered in the ambit of 5000-300 cm^{-1}on a Perkin-Elmer spectrum one, Perkin Elmer Fourier Transform Infra-Red (FTIR). UV-Vis spectrophotometer double beam PC 8 Auto Cell, Scanning Electron Microscope (SEM) of the Model Oxford INCAX Act, Transmission Electron Microscope (TEM), X-ray Diffraction (XRD) MiniFlex model, photoluminescence spectrophotometer.

3.2.1. Experimental Procedures

3.2.2. Production Extract Using Plant Seeds

The plant that was used for the synthesis of nanoparticles: Peganum Harmala seed, the seed are thoroughly rinsed with ionized distilled water, we let it dry until there was not a drop of water left in the heat of the air, after drying completely, it was ground with Dry Food Grinder Machine and Coffee Bean Grinder. We weighed 5 grams of ground seeds and dissolved them in water, then completed them with filtered water and let them mix for 2 hours on a magnetic stirrer without heat, the same ratio used with methanol and ethanol. The extracted mixture was filtered using quantitative filter paper No. 102 Medium, the filtered extract water, was kept for only three days during the process, but both the filtered methanol extract and the ethanol extract were kept for over a month at room temperature.

3.2.3. Synthesis of silver nanoparticles at 25 ℃

The silver nitrate solution was prepared at a concentration of 0.1 molars in 100 ml of distilled water, then we prepared three dilute solutions of concentrations (0.1 mM, 0.2 mM, 0.4 mM) also in 100 ml of distilled water, then we mixed 20 ml of water extract with 100 ml of Silver nitrate per three concentration, at room temperature (25 ℃) at a ratio of 2:10 (v/v) under vigorous

stirring, on a magnetic stirrer for 24 hours, then we repeated the same process for the methanol extract and, and ethanol from began harmala, the color change was observed The first after 12 hours of nanoparticles changed color from pale yellow to red-brown and then changed to dark brown or black in 24 hours.

3.2.4. Synthesis of Silver-Cobalt nanoparticles at 25 ℃

The same procedure used for the synthesis of Silver-Cobalt nanoparticles (Ag-CoNPs) also at room temperature, we prepared 100 ml solution of different concentrations of both silver nitrate AgNO3 and Cobalt Nitrate hexahydrate ($Co(NO_3)_2.6H_2O$), the concentration varied from (0.1 mM, 0.2 mM, 0.4 mM) Plant of (water, methanol, and ethanol) extract was added to a varied equal concentration of predecessor mixture solutions. The reaction was carried at ratio 2:10 (v/v) plant extract to predecessor mixture solutions, under vigorous stirring. 20 mL of plant (water, methanol, and ethanol) extract added to 100 mL of 1:1 Ag^{+}: Co^{+2}solution mixture. The (Ag-CoNPs) synthesized by the changing solution color from yellow pinkish to reddish-brown color, after 24 hr under stirring.

3.2.5. Synthesis of Cobalt nanoparticles (CoNPs) Using plant extract at 25 ℃

Cobalt nanoparticles (CoNPs), are synthesized by preparing a 0.1 molar solution of aqueous cobalt nitrate hexahydrate ($Co(NO_3)_2.6H_2O$) from 100 mL of distilled water, then we prepared three dilute solutions at concentrations (0.1 mM, 0.2 mM, 0.4 mM), using a ratio of 2: 10 (v/v), we mixed 20 ml of water extract of Harmala seeds with 100 ml of dilute solutions cobalt nitrate hexahydrate, then mixed the solution vigorously for 24 hours continuously. The color of the reaction solution changed after 24 hours. The same procedure was utilized for both methanol and ethanol plant extract.

3.2.6. Separation of the Biosynthesized (Ag, Co and Ag-Co)NPs

The nanoparticles made from the extracted water, ethanol and methanol, were removed from the mixture by pouring the excess solution, and then washed with distilled water three times to get rid of unwanted and excess substances, so as not to be interfered with other biological processes, to remove the nanoparticles and We used an assembled centrifuge at 4500 rpm for 10 minutes. After collecting the particles, we let them dry at room temperature without applying heat. As for the nanoparticles prepared using methanol extract and ethanol together, we let them dry at room temperature because they were not washable and were attached to the vessel. All particles were left to dry at room temperature.

3.3. Characterization of Nanoparticles

A high-performance UV-Vis spectrophotometer was used, which carried out between 300-700 nm wavelength ranges [113]. Absorption measurements were made for all Nano samples in a colloidal form, and placed in a quartz cuvette in which the radiation travels for a distance of one cm through the solution and works with an accuracy of one nanometer so that we used water, ethanol, and methanol were used as blank. The characteristic technique described above is carried out using an aqueous dispersion of nanoparticles.

FT-IR analysis was performed on clean and dry nanoparticles to identify potential active groups that could support the presence of capping and settlement by plant extracts. FTIR Spectrometer One Spectrum Potassium bromide (KBr) pellet was used in a diffusion reflection for nanoparticles produced from water extract, and the salt plate NaCl to nanoparticles synthesized from ethanol and methanol extract. The surface shape of the images of the nanoparticles was recorded by scanning the Electron Microscope (SEM), which measures 5-13 mm at working distance, 5-10 kV high voltage, and Emission current are 75-80. The energy-dispersed X-ray spectrometer (EDX) operates at a high voltage of 127 KeV and 20 A currents. The morphology of nanoparticles was studied using the XRD. X-ray diffraction (XRD) measurements were performed on drop-coated films to define the crystalline state of the Ag, Co, Ag-Co nanoparticles. At room temperature, the scanning rate ranges from 100 to 800 in 2 hours.

The photoluminescence study, XRD, SEM, EDX analyses were carried out at MUNZUR UNIVERSITY Labs, Turkey Tunceli. For UV-Vis, an FTIR spectrophotometer was analyzed at Firat University.

3.4. Antimicrobial Activity

Antimicrobial activity of the methanol extracts of flower and petal parts of P. tomentosa was determined according to the disk diffusion method (Collins & Lyne, 1987) [Collins, C.M., Lyne, P.M. (1987). Microbiological methods Butterworths & Co. Ltd., London.]. Bacterial strains (Staphylococcus aureus ATCC25923, Escherichia coli ATCC25322) were inoculated in Nutrient Buyyon (Difco) and incubated at 35±1°C for 24 hours. Yeast strains (Candida albicans FMC17) were inoculated in Malt Extract Buyyon (Difco), dermatophyte fungi (Trichophyton sp.) were inoculated in Glucose Sabouroud Buyyon (Difco) and incubated at 25 ± 1°C for 48 hours. The culture of prepared bacteria, yeast and fungi in broth are respectively; Müeller Hinton Agar was inoculated into Sabouraud Dextrose Agar and Potato Dextrose Agar at a rate of 1% (106 bacteria / ml, 104 yeast / ml, 104 fungi / ml). After shaking thoroughly, 25 ml was poured in sterile petri dishes with a diameter of 9 cm and homogeneously of the medium was dispersed. The filter paper discs (6 mm diameter) for each of discs 100 µl of different extracts were impregnated, were added to the appropriate agar media inoculated with microorganism. Then, petri dishes were

stored at 40C for 2 h. The inoculated petri dishes were incubated at 37±0.10C at 24 h for bacterial strains and also at 25±0.10C at 72 h for yeasts and dermatophyta fungi. As a control, different standard discs were used for bacteria (Ceftriaxone 30 µg/disk) and yeasts (Nystatin 30 µg/disk). Dimethyl sulfoxide (DMSO) was used for negative control. Inhibition zones formed on the medium at the end of the period were evaluated in mm.

4. RESULT AND DISCUSSION

4.1. FTIR Analysis of the Ag, Co, Ag-Co Nanoparticles

For specified the functional groups that are attached to synthesize NPs we utilized FTIR spectroscope (Perkin Elmer model with one spectrum) for this reason. We utilized KBr spherule for dried NPs and NaCl plate salt for aqueous NPs at a spectral range of 200 to 4000 cm-1. Each nanoparticle has been compared with its extract and the results are discussed below.

4.1.1. FTIR Analysis of the Ag NPs using water extract

The spectrum below, indicate the functional group present in Ag nanoparticles, synthesized using P. Harmala seed water extract is explained in Figure 4.1.

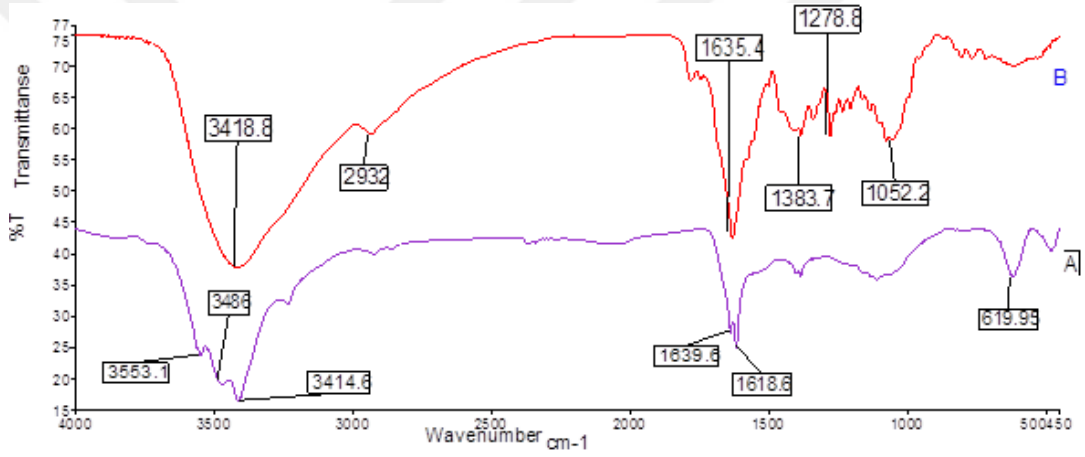

Figure 4.1: 1(a) Shows the FT-IR spectra of synthesized Ag, and (b) extract P.Harmala seed.

In order to identify the compounds responsible for the stabilization and reduction of silver nanoparticles, it is better to compare the spectra of the extract of Harmala seeds with those of the synthesized silver nanoparticles Ag NPs. Looking at the manuscript, the following peaks are noted: 3418.8, 2932, 1635.4, 1383.7, 1278.8, and 1052.2 cm^{-1}(for P.Harmala extract spectrum). The 3553.1, 3486, 3414.6, 1639.6, 1618.6, and 1412.7 cm^{-1} (for the Ag NP extract spectrum). The band at 3418.8 $cm^{-1}$for extracts and the band 3553.1, 3486, and 3414.6 cm^{-1} this three-band recorded for Ag NP are Indicates the presence of an OH and NH stretching of groups (phenols or hydroxyl groups or phenols or amines or amides of OH and NH respectively). Also, the peaks at 2932 for the extract of the plant indicate the expansion of C-H, and the absorption at 1635.4 for the extract and 1639.6 for the silver nanoparticle indicates the expansion of the carbonyl group C = O. The range 1618.6 cm−1 for AgNP is a function of the CN-terminal triple bond extension and C = C and the peaks at 1383.7 for the P. Harmala extract and at 1412.7 for silver nanoparticles are

a function of the CH bond. The range 1052.2-1060 $cm^{-1}$was indicative of the carbonyl groups in ether, alcohol, or carbon dioxide ester. According to [65] specific groups are responsible for reducing factors for nanoparticles, and as stabilizing factors, they are the phenolic group and the two groups CH and NH respectively, especially the two groups CH and NH The two groups correspond in proteins according to this report that stabilizes nanoparticles. FTIR studies confirmed that the carbonyl and amide flavonoid groups have the ability to encapsulate and stabilize silver nanoparticles, and have a strong affinity for metal ions [114].

4.1.2. FTIR Dissection of the Bimetallic Ag-CoNPs Using Water Extract

The figure below is the FTIR spectrum of the functional group in bimetallic Ag-CoNPs, which synthesized by P.Harmala seeds water extract, is appear in Figure 4.2.

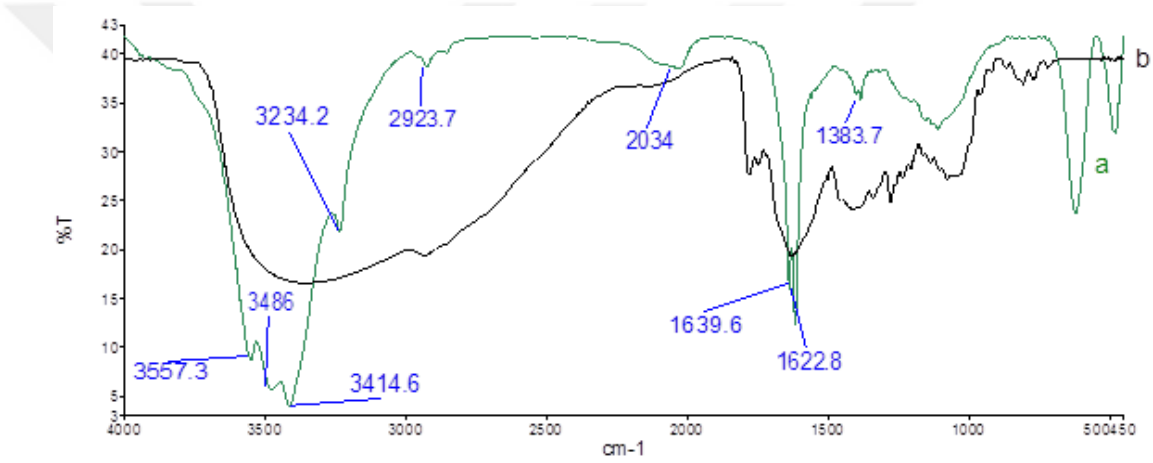

Figure 4.2: (a) and (b) are the FT-IR spectra of synthesized Ag-CoNP and extract P.Harmala seed respectively.

FTIR spectra of Ag-CoNP and P.Harmala seed extract are compared to identify the molecules responsible for the stabilization and reduction of the nanoparticles. Looking at the top chart we have peaks at 3565.6, 3334.59, 2932.7, 1627, 1404, 1275.8 cm^{-1} (spectrum of P.Harmala extract) and the other peaks are 3486, 3234.2, 2923.7, 1639.6, 1622.8, 1383.7 cm^{-1} (spectrum of Ag-CoNPs). The peak at 3565.6 cm^{-1} or 3334.59 cm^{-1} for extract and the band 3486 cm^{-1} or 3234.2 cm^{-1} for synthesized nanoparticles are referred to OH group stretching of (alcohol, phenols) and NH group of amine or amide.

Bands at 2932.7 cm^{-1} for extract are shifted to the band 2923.7 cm^{-1} for nanoparticle, referred to as CH stretching. The absorption spectrum 1627cm^{-1} for the extract and the absorption spectrum 1639.6 cm^{-1}, 1622.8 cm^{-1} for the nanoparticle, indicated to the C=N group. 1404 cm^{-1} band is for the extract is shifted to 1383.7 cm^{-1} for the nanoparticles referred to C-O group or –

CH_3 group. FTIR studies are confirmed that spotted peak mention up indicates the alkaloids and flavonoids that present in many plants are responsible for capping and stabilizing Ag-CoNPs.

Due to the presence of various organic substances in the plant extract, the peaks are multiple for nanoparticles made by plants. This is chemically different, usually showing a small number of strong peaks, as shown in (Figure 4.2a), (Figure 4.2b). This, of course, provided evidence of capping bio reducing agents (plant extracts) that further stabilizes nanoparticles.

4.1.3. FTIR to Clarifying of the synthesized CoNPs using water extract

The FTIR below, representing the functional group that responsible for reducing the CoNPs, which synthesized using P.Harmala seed water extract, is shown in Figure 4.3.

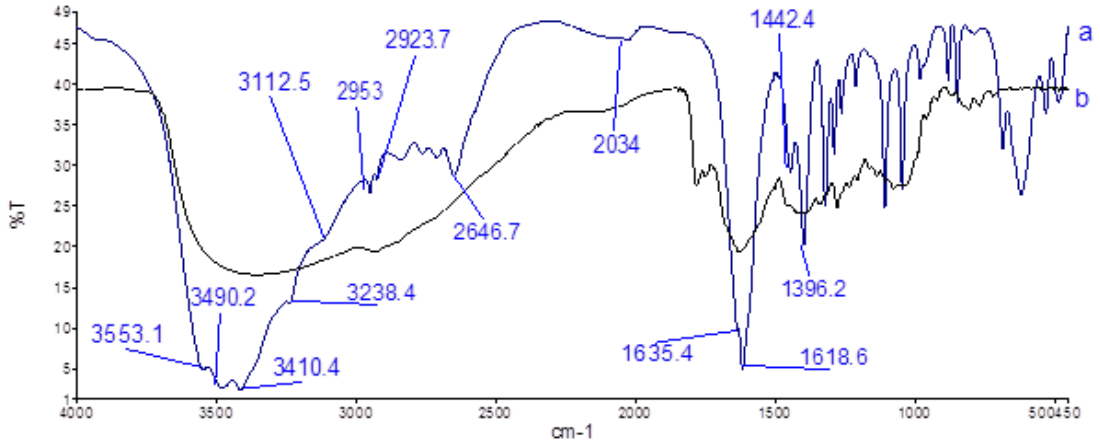

Figure 4.3: (a) and (b) are the FT-IR spectra of synthesized CoNP and extract P.Harmala seed respectively.

Looking at the spectrograph at the top shows the presence of peaks for cobalt nanoparticles at wave number 3490.2, 3410.4, 3238.4, 2923.7, 2646.7, 2034, 1618.6, 1396.2, and 1071 cm^{-1}, cause of the presence of flavonoids and phenols in a high degree in the plant extract, it is one of the reasons for the presence of the high antioxidants capacity. 3490-3238.4 cm^{-1} is equal to the band O-H. 3490-3238.4 cm^{-1} equals the O-H range. The peak appears at 2923.7 cm^{-1}-CH_2. The peaks of 1618.6 cm^{-1} refer to the carbonyl group.

The peak of 1396.2 cm^{-1} resembles the C=C of the aromatic or C-N of the aromatic amine and the peaks have drawn at 1070 cm^{-1} indicate the C-N expansion in carboxylic acids, ethers, alcohols, and esters. According to the spectroscopic results, it can be concluded that polycyclic compounds such as alkaloids and flavonoids act as insoluble in water responsible for the reduction and stabilization of cobalt nanoparticles. The FTR spectrum of Peganum Haramala extract showed the groups that usually convert cobalt ions into cobalt nanoparticles [115,116].

4.1.4. FTIR Analysis of the AgNPs using methanol extract

The spectrum below, represent the functional group present in Ag nanoparticles, synthesized using P.Harmala seed methanol extract is showed in Figure 4.4.

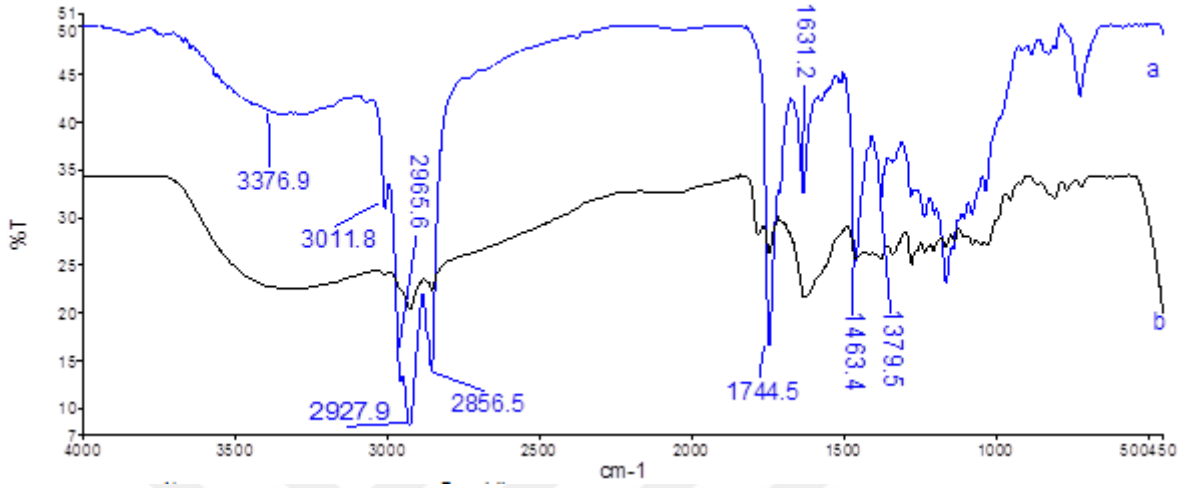

Figure 4.4: (a) and (b) are the FT-IR spectra of synthesized AgNP and methanol extract P.Harmala seed respectively.

The methanol extract of P.Hramala and AgNPs spectra are compared to understand the synthesized AgNPs functional groups. Figure 4.4 shown the peak at 3376.9, 3011.8, 2928, 2856.5, 1744.5, 1631, 1463.4, and 1379.5 cm^{-1}, the broad peak 3376.9cm^{-1} assigned to the O-H group. The band 2928-2856.5cm^{-1} corresponds to C-H, the band 3011.8 cm^{-1} due to C=C may be. The acute peak at 1631.2 cm^{-1} indicates aromatic C=N. The C=O extension refer to ester was shown at 1744.5 cm^{-1}, and the –C-H extension and the C-O disfigurement were observed at 1379.5 cm^{-1} and 1165.2 cm^{-1} respectively. The peaks observed at FTIR were characteristic of the abundant alkaloids of the Peganum Harmala seeds. The result suggests that the alkaloids may be responsible for the reduction of Ag^{+} ions to Ag^{0}.

4.1.5. FTIR Analysis of bimetallic Ag-Co nanoparticles using methanol extract

The figure below Figure 4.5 are shown the result of spectrum for synthesize of Ag-CoNPs.

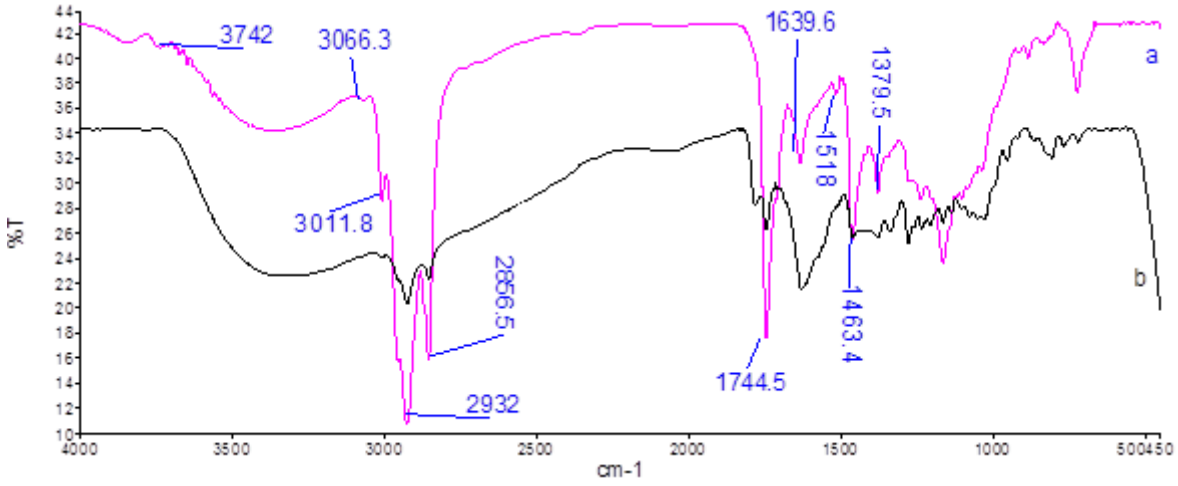

Figure 4.5: (a) and (b) are the FT-IR spectra of synthesized Ag-CoNP and methanol extract P.Harmala seed respectively.

According to the spectrum, peaks that achieved bimetallic Ag-CoNPs were 3426 cm^{-1} (OH stretch), 2932-2856.5 cm^{-1} (CH stretch), 1744.5 cm^{-1} (C=O), 1639.6 cm^{-1} (C = N), 1463.4 cm^{-1}, 1379.5 cm^{-1} (-CH) and 1165 cm^{-1} -CO, those value of absorption peaks, submit the existence of phytochemicals component on the outer side of the Nanohybrid via OH, which has lost hydrogen ions to interact with the metal precursor mixture.

4.1.6. FTIR Analysis of the Co nanoparticles using methanol extract

Representative FTIR spectrum of Co nanoparticles synthesized by P.Harmala seed using methanol extract, presented in Figure 4.6.

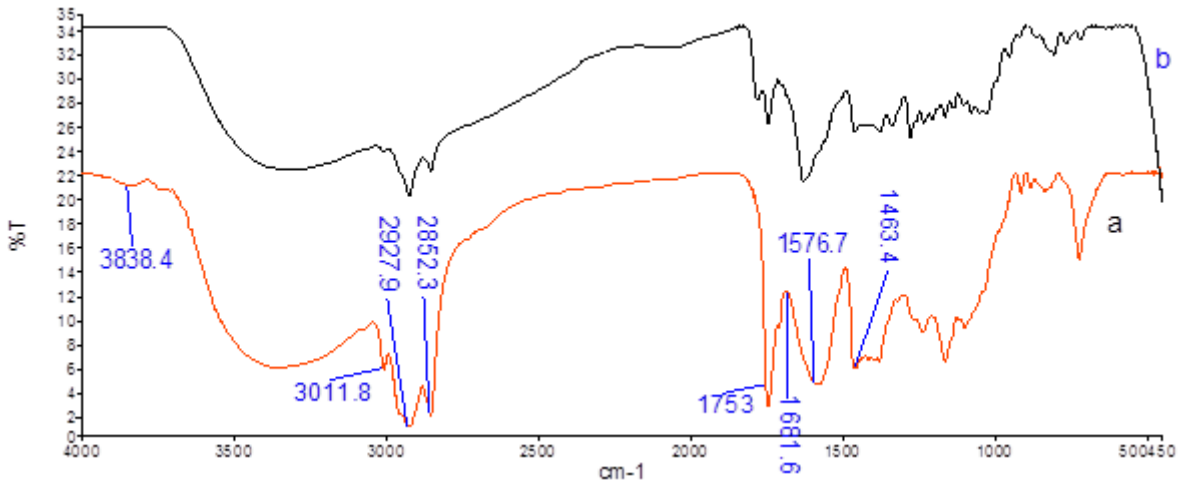

Figure 4.6: (a) and (b) shows the FT-IR spectra of synthesized CoNP and methanol extract P.Harmala seed respectively.

The FTIR spectrum shows that bioactive chemicals capped the nanoparticles at 3369.4, 2927.9, 1753, 1576.7, 1463.4, and 1161.3 cm^{-1} with hydroxyl group (OH) stretch, (CH) stretch, C=O, -NH or NH_2 stretch, and It showed the presence of CO group. Each screening for phytochemicals showed the presence of alkaloids and saponins components of Peganum Harmala methanol extract. The nanoclusters were covered with alkaloids present in phytochemicals to provide stability.

4.1.7. FTIR Spectrum Analysis of Three NPs (Ag, Co, Ag-Co) Using Ethanol Extract

The result of FTIR spectrum indicates the functional groups presented in three NPs (Ag, Co, Ag-Co), synthesized by P.Harmala seed using ethanol extract, recorded with in the wavenumber range 4000-450 cm-1, the result showed in Figure 4.7.

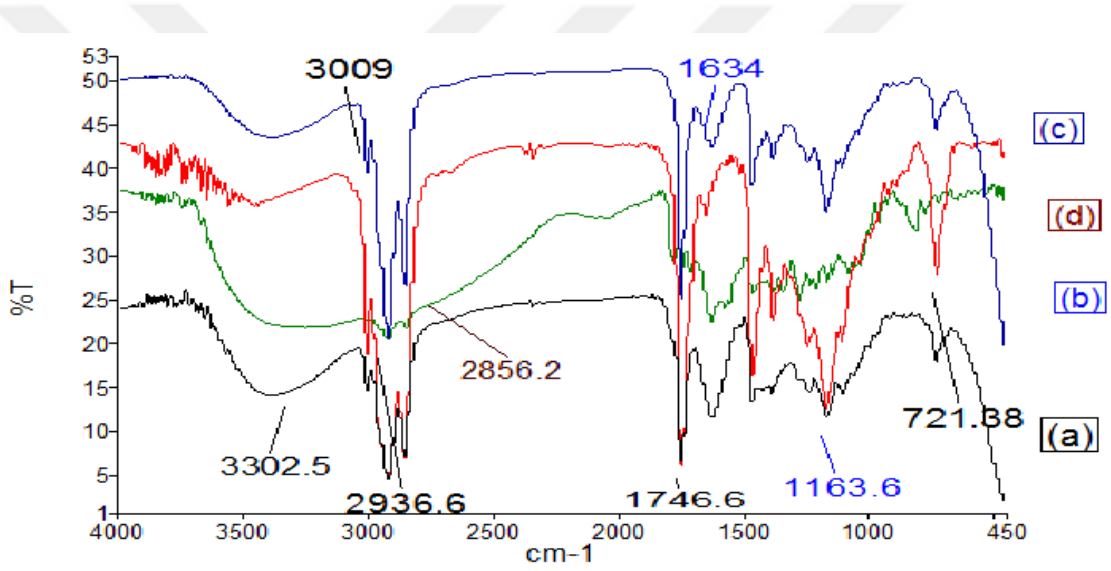

Figure 4.7: The FT-IR peaks of synthesized NP shows (a) AgNPs, (b) Ag-CoNPs, (c) CoNPs and (d) ethanol extract P.Harmala seed.

The results are refers to three different nanoparticles synthesized in the presence of the studied extract analyzed and indicates the absorption peaks that are conformed the functional group responsible of capping extracts (Ag, Co, Ag-CoNPs). The synthesized extracts and extracts (Ag, Co, Ag-CoNPs) show peak positions and some peaks that are missed, which obviously showing the existence of reminding plant extracts in the reducing composition. At frequencies around 3302.5, 3009, 2936.6, 2856.2, 1746.6, 1634, 1163.6, and 721.3 cm^{-1}, a shift of the peak with a decreasing band or increased intensity was observed, resulting in hydroxyl, alkene ($=CH_2$), alkyl ($-CH_3$, $-CH_2-$), C=O ester or aldehyde, amide (NH), $-OCH_3$ and aromatic H substituent groups, each peaks conform the stretching groups, those groups were responsible of capping the silver, cobalt, silver-cobalt nanoparticles [117], [1].

4.2. **Analysis by Ultra-Violet visible Spectroscopy**

To evaluate the size and shape of nanoparticles in a solution of cloudy extracts, the ultraviolet spectroscopy technique is utilized for this reason [118]. Ag, Co, Ag-CoNPs synthesized by various solvent extracts were evaluated by UV-wave analysis. The difference in physical intensity manifested by the pale black color (confirmation of the formation of AgNPs and Ag-CoNPs) and the reddish-brown (confirmation of the formation of CoNPs)Using different solvents to extract the seeds, the nanoparticles Ag, Co, Ag-Co offered various reductions according to their reducing abilities. It is a renowned fact that Ag NPs display different colors depending on their bulk and shape [119]. First, in a conical flask with a volume of 100 ml, a solution of silver nitrate was prepared at a concentration of 0.1 M. Then three dilute solutions of silver nitrate that were previously banned were made with various concentrations of (1-4 mm) and 5, 15 and 20 ml of different solvent extracts of Pegnum Harmala seeds were added each unit in a different container to the $AgNO_3$ solution. The process was previously repeated for the synthesis of the cobalt and silver-cobalt bimetallic particles.

By using the UV spectrum, we examined the reduction process at different time intervals. Among the results we obtained, we chose the spectral results of the higher concentrated solution because they gave better spectra than the less concentrated ones. The following figure shows a comparison of Peganum Harmala extract with water, ethanol, and methanol, followed by a comparison of synthetic Ag nanoparticles, Co nanoparticles, and Ag-Co nanoparticles from different solvent extracts.

4.2.1. UV-Vis spectroscopy analysis for Peganum Harmala seed extract

Figure 4.8 depicts the absorption spectra of the Peganum Harmala seed extracted with methanol, ethanol, and water it was recorded with a UV-VIS spectrophotometer at 25 °C. The recorded absorbance data are offered in Table 4.1.

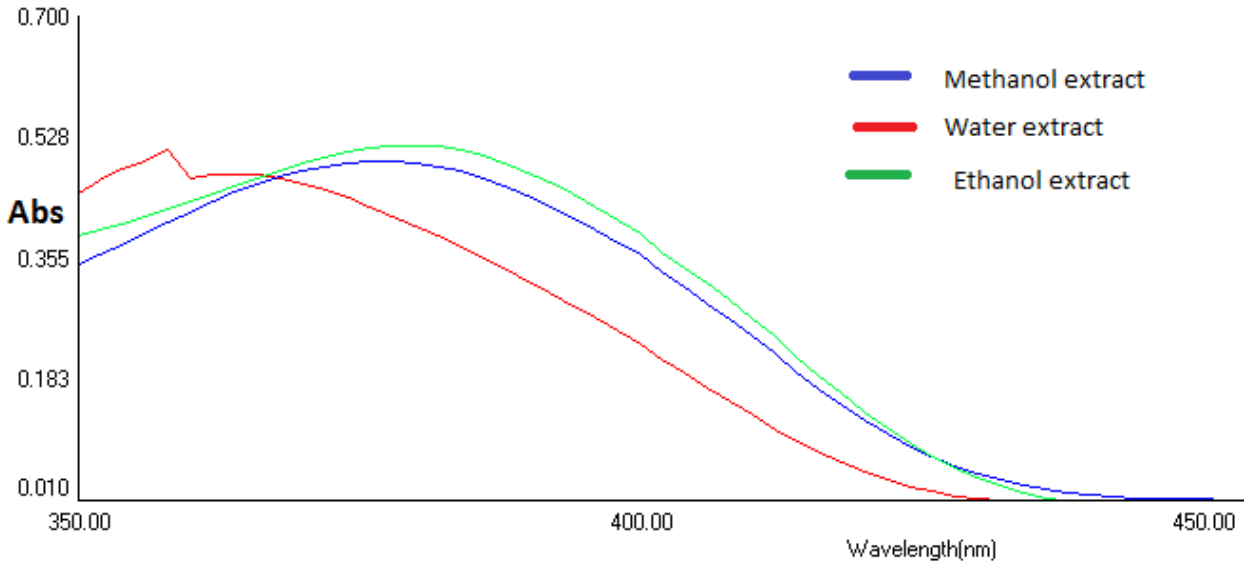

Figure 4.8: The UV-Vis spectra of three extracts of Harmala seeds, prepared at room temperature.

Table 4.1: Parameters of Peganum Harmala seed extract in three different solvent

Peganum Harmala seed extract	Maximum Abs	Maximum Wavlength(nm)
Methanol extract	0.476	364
Ethanol extract	0.494	380
Water extract	0.517	376

From Figure 4.8, we can see that the absorption peaks that characterize the Peganum Harmala extraction in the three solutions are different. The Peganum Harmala extract in water is characterized by one major absorption peak located at 376 nm, whereas for ethanol and methanol their absorption peaks are 380 nm and 364 nm, respectively. In fact, we used the same concentration of Peganum Harmala seeds. The absorption peak increases with decreasing particle size [120]. The position of the maximum intensity was highly dependent on the used solvent [121].

4.2.2. UV-Vis spectroscopy analyezis of (silver, cobalt, silver-cobalt nanoparticles) using Peganum Harmala seed in three different solvent as extract

Figure 4.9. Are offered the UV–visible spectra that absorbed by Ag, Co, Ag-Co nanoparticles synthesized by Peganum Harmala seed water extracts.

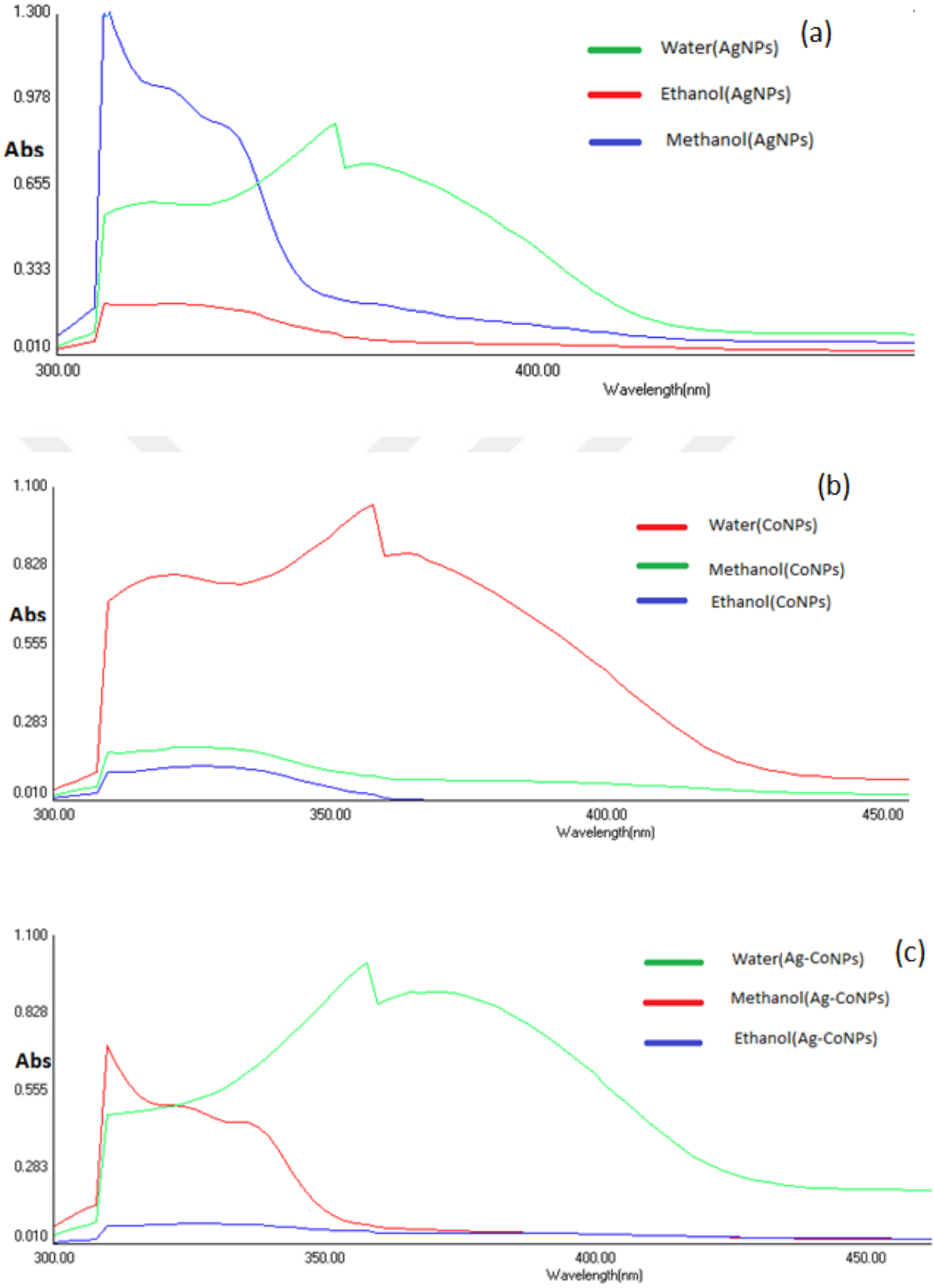

Figure 4.9: UV–vis spectra of the synthesized (a) AgNPs using water, methanol and ethanol, (b) CoNPs using water, methanol and ethanol and (c) Ag-CoNPs using water, methanol and ethanol of Peganum Harmala seed.

(a) (b) (c)

(d) (e) (f)

(g) (h) (i)

Figure 4.10: (a) $AgNO_3$ solution, water extract of plant before reduction and silver dispersion formed after reduction, (b) Ag-CoNPs with CoNPs (WE), (c) Ag-CoNPs formed in different concentration (WE), (d) $AgNO_3$ with methanol extract (ME), (e) $AgNO_3$ with ethanol extract (EE), (f) AgNPs formed after reduction (ME), (g) $Co(NO_3)_2.6H_2O$ with extract (EE), (h) Ag-CoNPs formed after reduction of both (ME), (EE), (i) AgNPs formed after reduction of (EE).

Table 4.2: The absorption result with wavelength of Ag, Co, Ag-CoNPs, with three different solvents.

NPs	Maximum Abs	Maximum Wavelength(nm)
Ag+W	0.728	366
Co+W	1.033	358
Ag-Co+W	0.900	366
Ag+M	1.371	310
Co+M	0.194	326
Ag-Co+M	0.080	326
Ag+E	0.200	324
Co+E	0.127	326
Ag-Co+E	0.709	310

In (Figure 4.10). The formation of the three nanoparticles in each of the germinated seed extracts was observed optically due to the obvious change in their color during the particle formation process, whereby Ag and Ag-CoNPs gave a clear change from water color to dark brown color and brown color Reddish for CoNPs.

We have put the results in the top table according to the maximum absorption result (λmax) for each of the nanoparticles, which are called SPR. By looking at the results, silver particles presented the highest absorption peaks at 310 to 366 nm, and the SPR (max) absorption peak for cobalt particle was from 326 to 358 nm and for silver cobalt bimetallic nanoparticles from 310 to 366 nm as shown in Table 4.2. The intensity of the SPR peak for AgNP composed of ethanol and methanol extract was lower than that of the water extract due to incomplete reduction or macromolecules. Silver nanoparticles synthesized using the water extract of Peganum Harmala have sharp and strong SPR peaks and a large number of high-density nanoparticles that increase the strength of the absorption band as shows in Fig. 4.9 (a) [122]. It was found that the solvent was used in the extraction of Peganum Harmala, which affected how the particles formed for silver nanoparticles and controlled their shape and how they spread according to the solvent used in their manufacture [123]. This is evidence that different solvents play a major role in how the nanoparticles are sized and how the optical properties of silver nanoparticles are [117].

The surface plasmon resonance of cobalt nanoparticles is unique according to the absorption peaks given, where UV-Vis recorded the maximum absorption peak recorded at 358 nm for the water extract. Considering the results, the intensity of SPR peaks for CoNPs prepared from water extract is greater than that obtained from ethanol and methanol extract. The UV absorption spectrum of the prepared nanoparticles with aqueous extract of Peganum Harmala

Has a wavelength shift, and the bandwidth increases with decreasing the nanoparticle radius [124]. UV-Vis absorbance spectroscopy is so sensitive to a particle size that it has become a useful technique for investigating the shape and location of absorbance peaks. Also, nucleation

and onset growth of CoNPs were delayed by up to 24 hour of reaction, unlike the synthesis of AgNP, which started as early as 1hrs. The reaction conditions at room temperature were not compatible for the synthesis of cobalt nanoparticles using three solvents as extract of Peganum rue seed to act as a reducing and stabilizing agent. This may be due to the interaction that occurs between the biomolecule and the synthesized nanoparticles. Although the reaction occurred at room temperature, the color change observed within 24 hours indicates the formation of nanoparticles and the change of Ag^{+} to Ag^{0}. The surface plasmon resonance results of AgNP nanoparticles provided the maximum absorption wavelength (Fig. 4.9(d)). The absorption peaks of the synthesized Ag-CoNPs water extract showed stronger intensity and bandwidth than the ethanol and methanol extracts, with peaks at 310 and 326 nm, respectively. Under these reaction conditions, the presence of Co in the hybrid produced the absorption wavelengths (326-358 nm) observed in the Ag-CoNP spectrum, whereas the corresponding single metal AgNPs had absorption wavelengths of 310-366 nm. The discrepancy may be cause of overlapping electronic conditions of the bimetal component leading to changes in SPR [125].

4.3. X-ray diffraction (XRD) analysis

For more information on how silver, cobalt, silver, and cobalt nanoparticles were synthesized from P. Harmala seed extract by XRD images. We were unable to take cobalt and silver nanoparticles of the methanol extract and silver and cobalt nanoparticles of the ethanol extract due to the humidity of the sample. In the figure below, the structure of nanoparticles is shown.

4.3.1. X-ray diffraction analysis of (Ag, Co, Ag-CoNPs) of water extract

Figure 4.11shows the XRD patterns of Ag, Co and Ag-Co bimetallic NPs formed using aqueous extract of P.Harmala seeds at room temperature. XRD results for silver nanoparticles at(**Figure 4.11**(a)) the reflectance peak at 2θ values of 27.78, 32.00, 38.00, 44.41, 46.21, 54.83, 57.44 and 77.01 corresponding to the reflections of (362), (744), (297), and (108), (468), (123), (124) and (209) respectively; Which shows the shape of the crystalline cubic Ag particles. Simultaneously, **Figure 4.11**(b) shows the 2θ values of the Co diffraction peaks at 13.40, 15.53, 23.17, 25.26, 28.65, 32.66 and 41.17 degrees corresponding to (192), (295), and (118). (121) and (148), (163) and (151). From the XRD pattern Co molecules maintain their crystalline structure during formation [126].

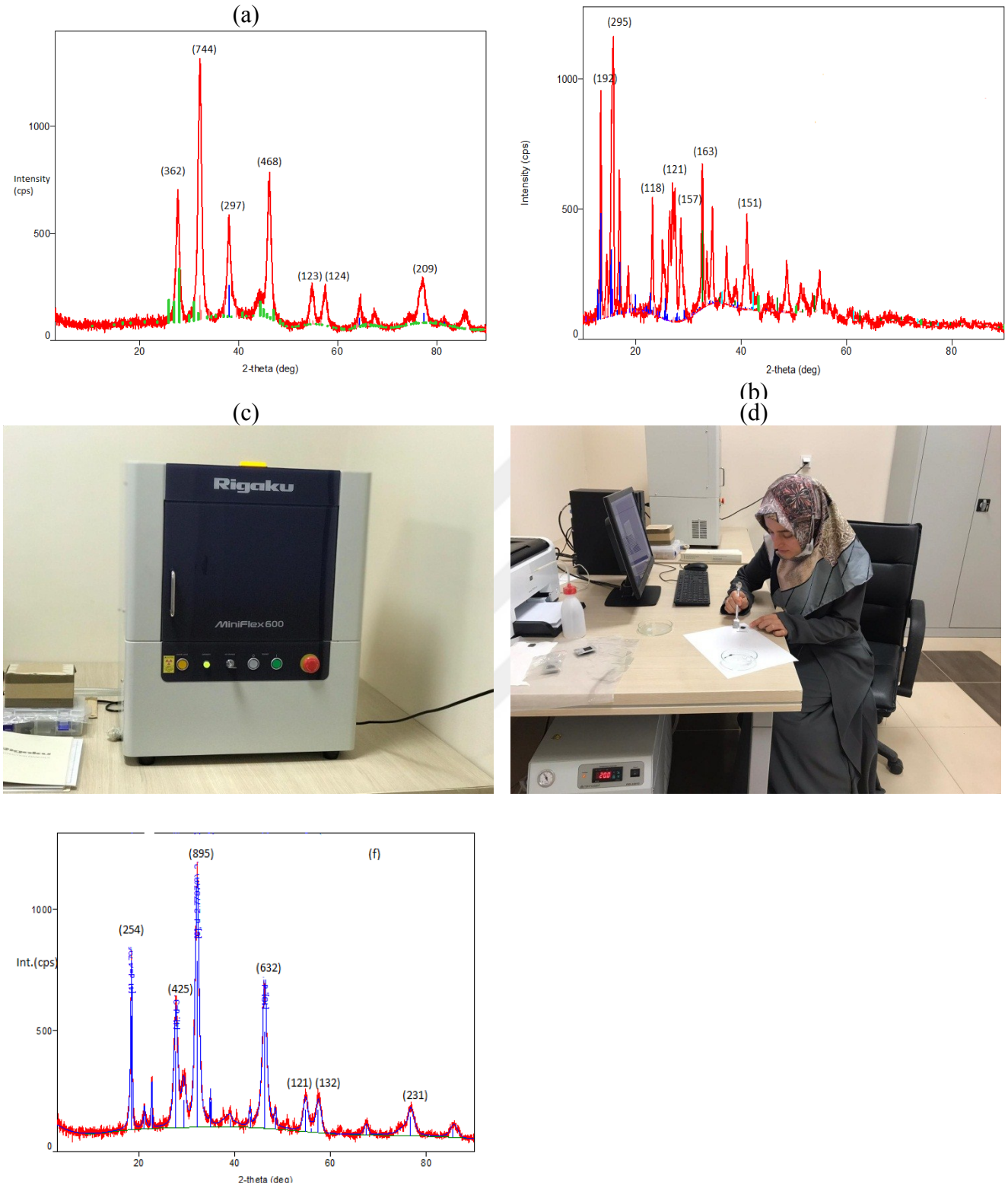

Figure 4.11: The XRD patterns of (a) Ag, (b) Co, and (f) Ag-Co bimetallic nanoparticles formed with the water extract of P.harmala seed. (c) XRD machine, (d) Sample of nanoparticles.

The powder sample was used for XRD analysis to confirm the presence of Ag-CoNPs. According to (**Figure 4.11** (f)), Diffraction was performed over 10-80. Eight reflectance peaks with 2θ values were observed at 18.48, 27.75, 29.39, 32.17, 46.23, 54.74, 57.43, and 76.62 crystal levels corresponding to the inversions of (254), (485, (159), (895), (632) and (121) and (139) and (231). The diffraction pattern indicated the Co, Ag peaks, and it showed that the Ag-Co hybrid structure is morphological for the nucleus shell.

4.3.2. X-ray diffraction analysis of (Ag, CoNPs) of ethanol extract

An investigation of the crystallinity of silver and cobalt nanoparticles prepared using ethanol extract of P. Harmala seed is shown in Figure 4.12.

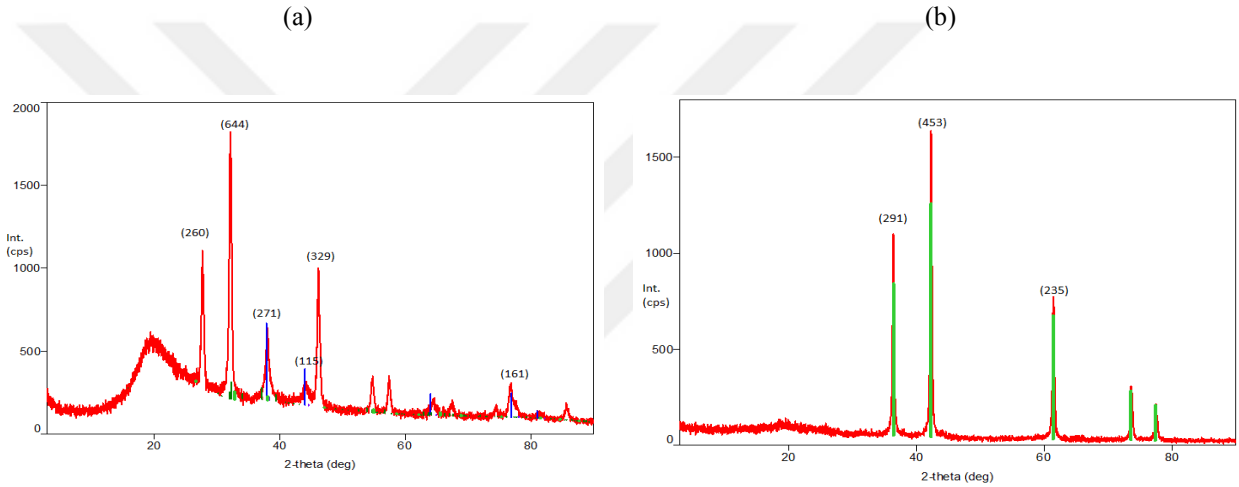

Figure 4.12: The XRD patterns of (a) Ag, and (b) CoNPs formed with the ethanol extract of P.harmala seed.

X-ray diffusion samples were studied to verify the angle condition and crystalline shape of Ag NPs synthesized from P. Harmala ethanol extract. The crystal shape in XRD is consistent with the Bragg reflections and this, in turn, corresponds to the formation of FCC silver. (Figure 4.12(a)) shows XRD samples of Ag NPs synthesized from P.Harmala extract using ethanol as solvent. The peaks shown at the values of 2θ are 27.74, 32.16, 38.06, 44.14, 46.17, and 76.71 with respect to the (260), (644), (271), (115), (329), and (161) planes. The studied XRD data showed that the composition of Ag NPs was a composite imprint crystal [117]. Also, **Figure 4.12**(b) presents the 2θ values of the Co diffraction peaks at the 36.40, 42.29, and 61.40 crystalline levels corresponding to the (291), (453), and (235) reflections corresponding to the face-centered cubic crystal phase of cobalt.

4.4. Analyzing Nanoparticles by Scanning electron microscopy (SEM), and Energy dissipation spectroscopy (EDS)

The surface morphology and composition of Ag, Co, Ag-CoNPs synthesized by P. Harmala extracted in (water, methanol, and ethanol) as solvent, were analyzed by SEM using EDX analyses. The EDX device can be used to learn how to structure and distribute molecules in nanoparticles, via graphs and spectroscopy, which are integrated with scanning electron microscopy (SEM) [117]. The synthesis of nanoparticles by both methanol and ethanol was adhesive and non-dryable due to this, we were not able to analyze both Ag-CoNPs (EE) and AgNPs (ME).

4.4.1. SEM analysis, and EDS analysis for Ag, Co, Ag-CoNPs

In (Figure 4.13) shows through SEM morphological images of AgNPs made by water extract of P. Harmala. Their particles are cubic shapes. Also (Figure 4.14), and (Figure 4.15) showed the morphological character for both CoNPs and Ag-CoNPs respectively. The SEM images of CoNPs showed spherical shapes the Ag-CoNPs cubic shapes.

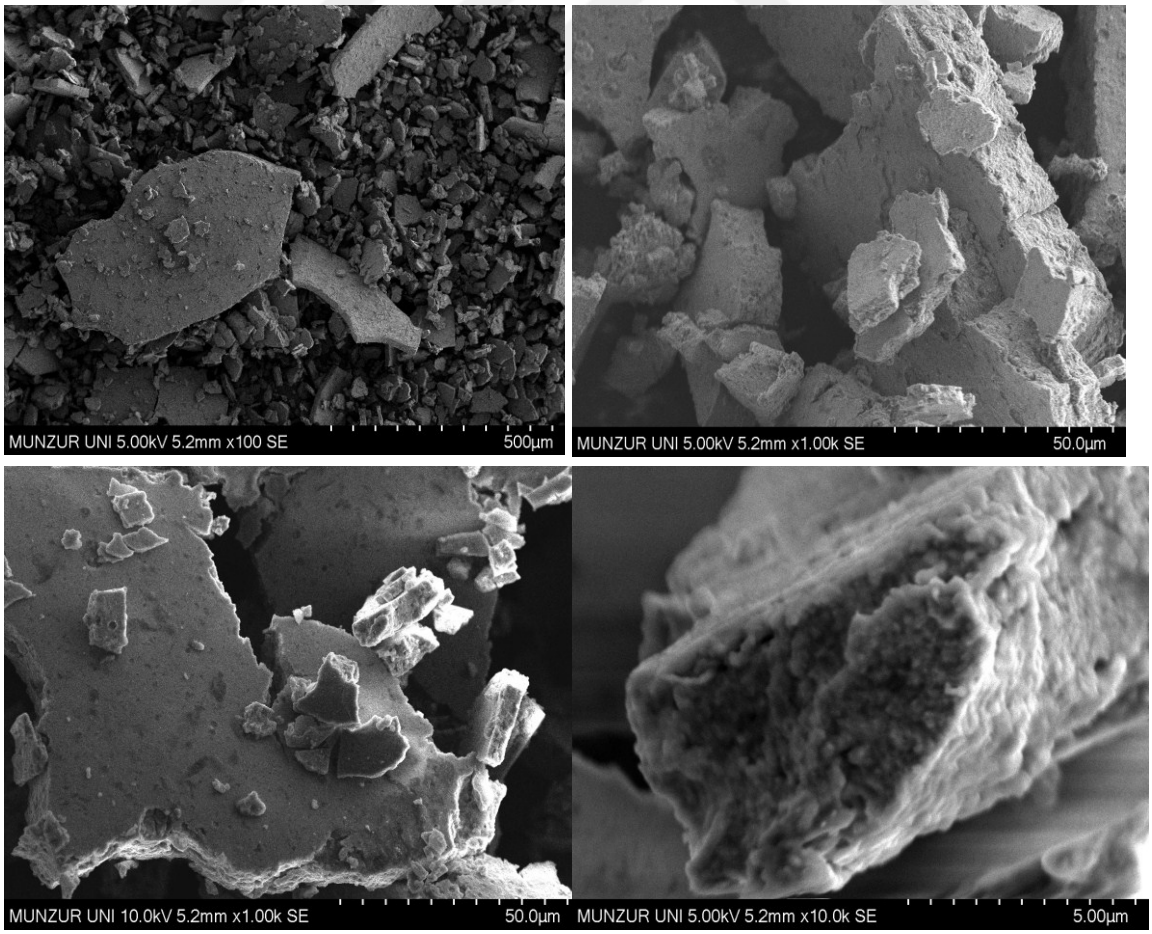

Figure 4.13: SEM image of silver nanoparticles synthesied by P.Harmala (WE) at different magnification levels**.**

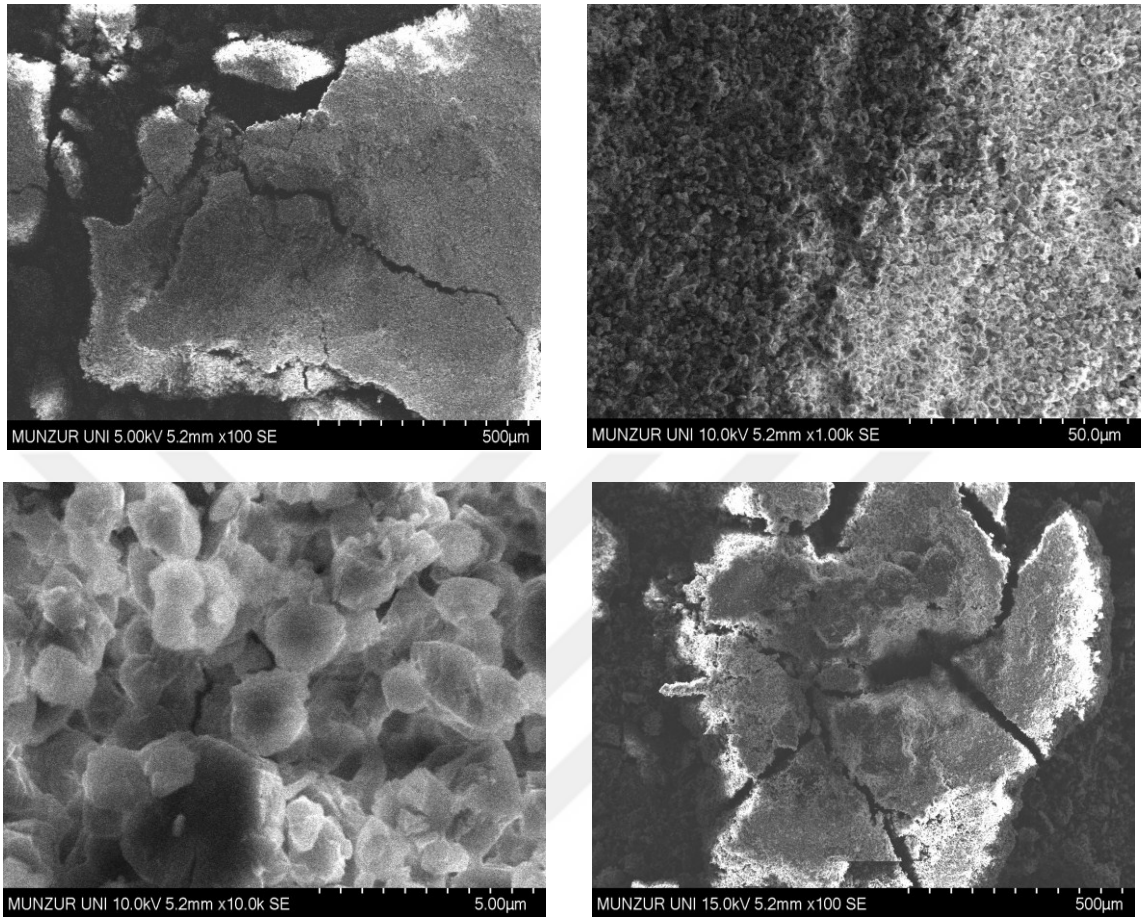

Figure 4.14: SEM image of cobalt nanoparticles synthesied by P.Harmala (WE) at different magnification levels.

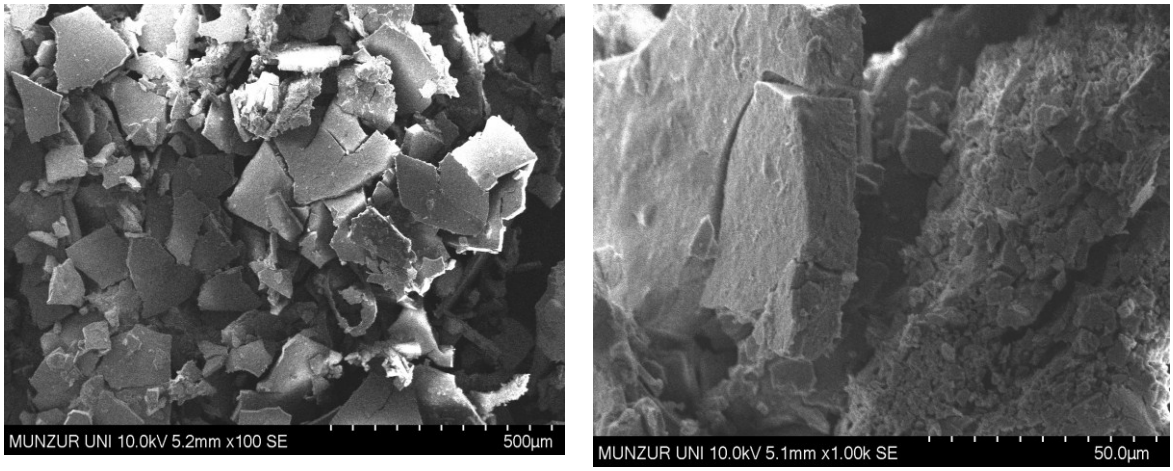

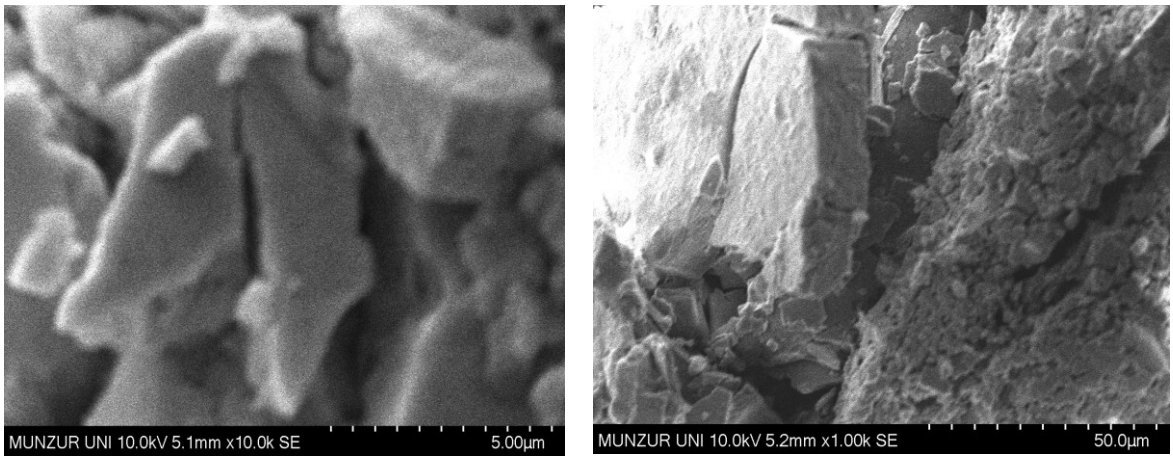

Figure 4.15: SEM image of silver-cobalt nanoparticles synthesied by P.Harmala (WE) at different magnification levels.

Elemental mapping analysis of silver nanoparticles reveals a significant diffusion of metallic silver in a scanning electron micrograph of silver nanoparticles (Figure 4.16 a and b). The EDX profile (Table 4.3) shows a massive silver mark with little oxygen in addition to the carbon signal, which may have come from biomolecules that were, attached to the AgNPs particles. Some weak signals for C, P and Au were also observed.

(a) (b)

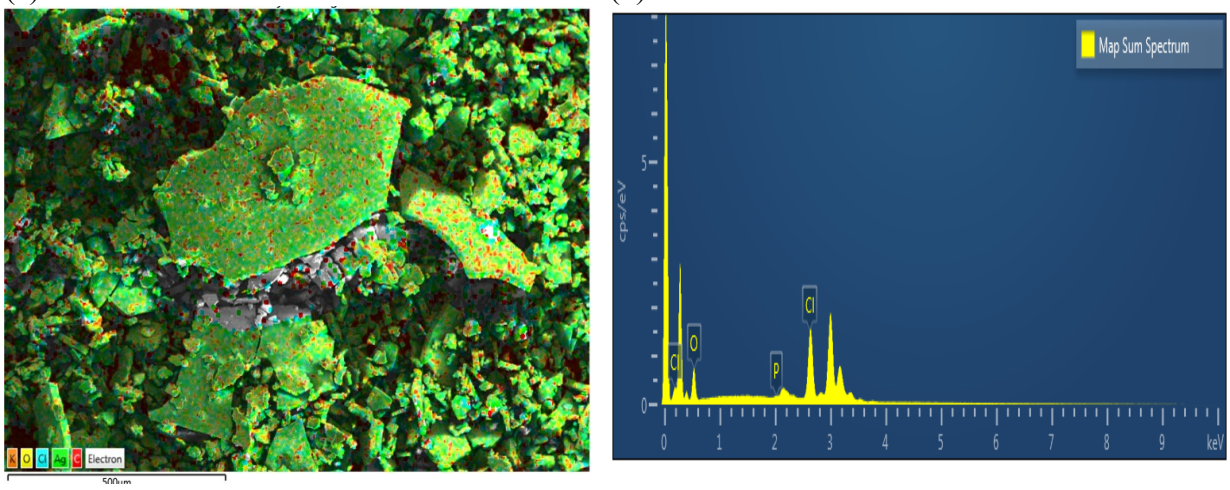

Figure 4.16: EDX spectrum of silver nanoparticles (a), spreading of silver element. (b), electron micrograph region of silver nanoparticles.

Table 4.3: EDX measurement of the atomic content in AgNPs synthesized in room temperature (WE).

Map Sum Spectrum				
Element	Line Type	Weight %	Weight % Sigma	Atomic %
Cl	K series	11.03	0.11	8.83
Ag	L series	50.56	0.28	13.31
O	K series	9.46	0.16	16.79
Au	M series	3.24	0.24	0.47
C	K series	25.58	0.21	60.47
P	K series	0.14	0.05	0.13
Total		100		100

Elementary mapping analysis of cobalt nanoparticles reveals a low assignment of metallic cobalt as a scanned electron micrograph of cobalt nanoparticles (Figure 4.17a and b). Also, the EDX analysis showed that a small amount of Co with the atomic structure was 14.74% in the constituent nanoparticles (Table 4.4).

(a) (b)

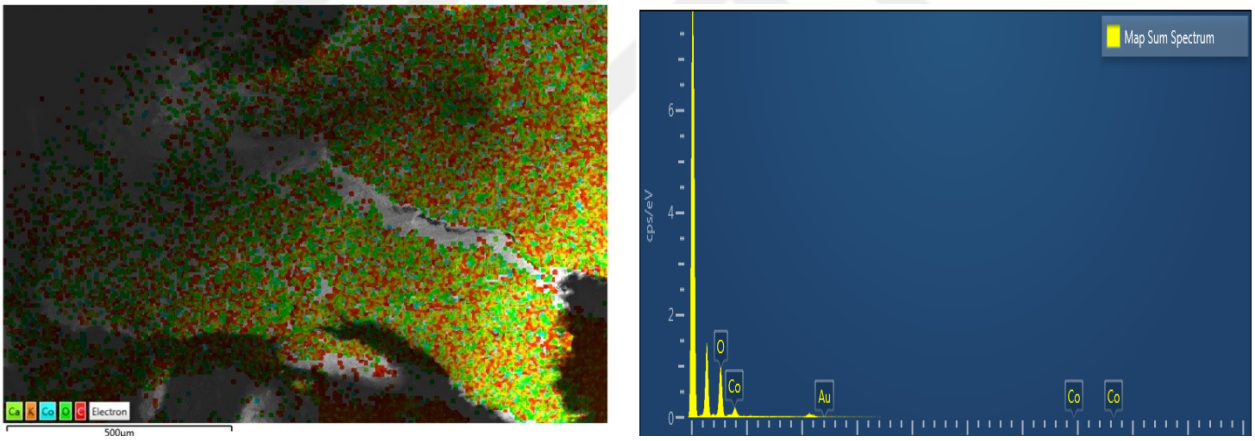

Figure 4.17: EDX spectrum of cobalt nanoparticles (a), dispearing of cobalt element. (b), electron micrograph area of cobalt nanoparticles.

Table 4.4: EDX measurement of the atomic content in CoNPs synthesized in room temperature (WE).

Map Sum Spectrum				
Element	Line Type	Weight %	Weight % Sigma	Atomic %
C	K series	35.87	0.77	56.41
O	K series	31.46	0.71	37.15
Co	L series	14.74	0.74	4.73
Au	M series	17.93	1.38	1.72
Total		100		100

Elemental mapping analysis of silver and cobalt nanoparticles reveals a high proportion of metallic silver scattered in the scanned electron microscopy imaging image but without any appearance of metallic cobalt for a solution of silver and cobalt nanoparticles (Figure 4.18a and b). The EDX analysis indicated that there was a greater amount of Ag in the bimetallic particle structure by 50.71%, and 0.00% in the amount of cobalt in the synthesis (Table 4.5).

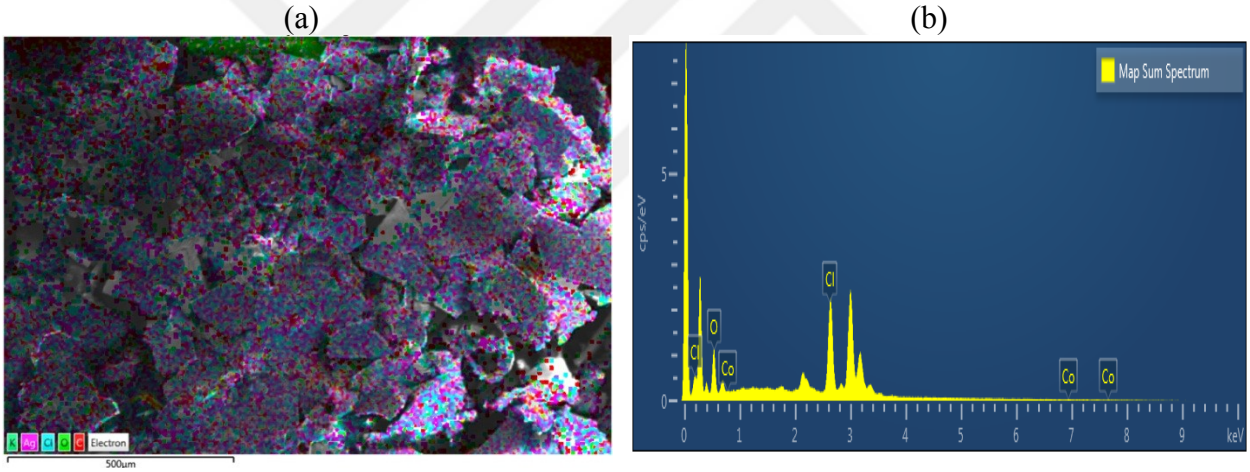

Figure 4.18: EDX spectrum of silver-cobalt nanoparticles (a), distribution of silver-cobalt element. (b), elemental mapping: electron micrograph area of silver-cobalt nanoparticles.

Table 4.5: EDX measurement of the atomic content in Ag-CoNPs synthesized in room temperature (WE).

Map Sum Spectrum				
Element	Line Type	Weight %	Weight % Sigma	Atomic %
C	K series	20.17	0.30	51.99
O	K series	11.09	0.25	21.46
Cl	K series	12.39	0.17	10.82
Ag	L series	50.71	0.41	14.55
Au	M series	5.33	0.33	0.84
Si	K series	0.30	0.05	0.33
Co	L series	0	0.31	0
Total		100		100

4.4.2. SEM and EDX analysis of Ag, and CoNPs of ethanol extract

In (Figure 4.19) SEM reveals the morphological nature of AgNPs produced utilizing P. Harmala seeds ethanol extract at room temperature. From the perspective of the picture, the Nanoparticles are cubic shapes. While **Figure 4.20** showed the morphological character for CoNPs, the SEM images of CoNPs showed spherical shapes.

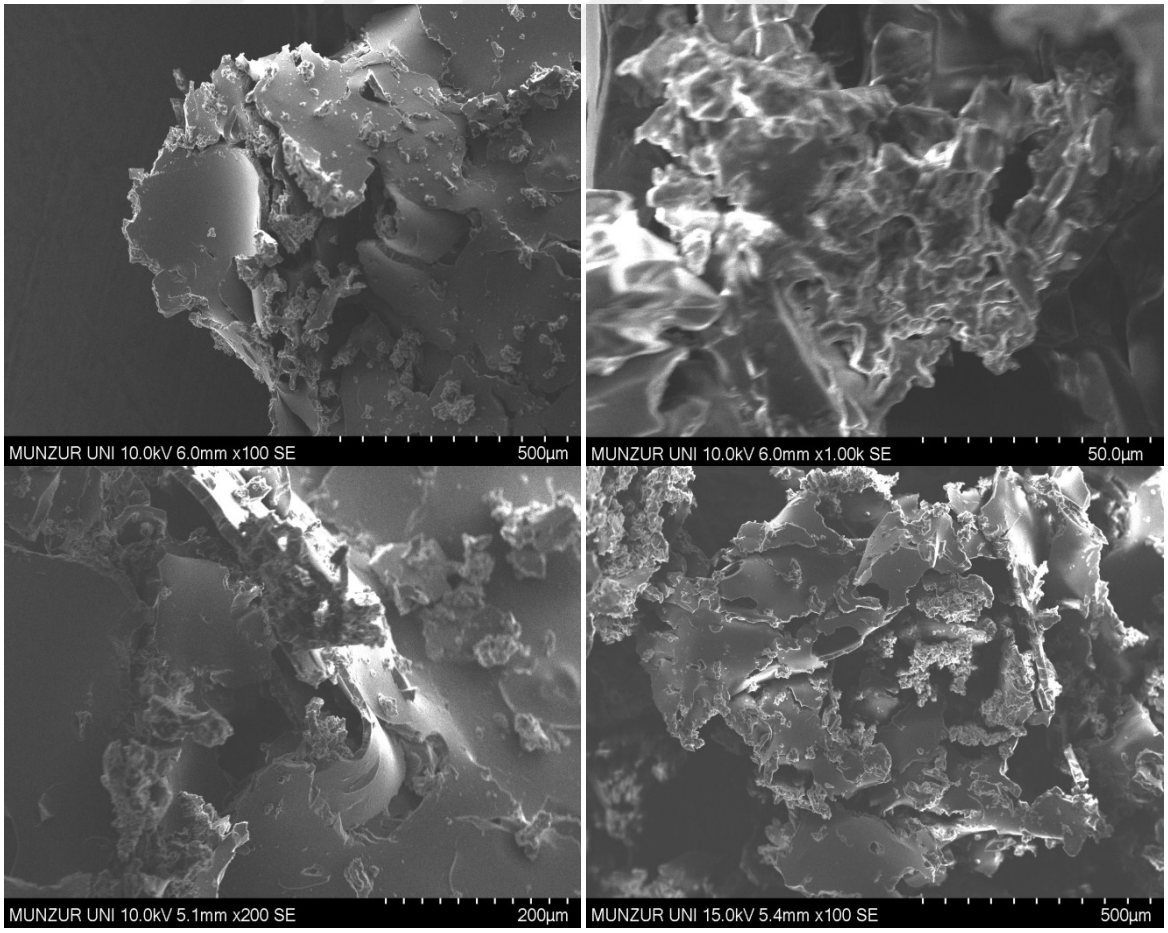

Figure 4.19: SEM image of silver nanoparticles synthesied by P.Harmala (EE) at various enlargement levels

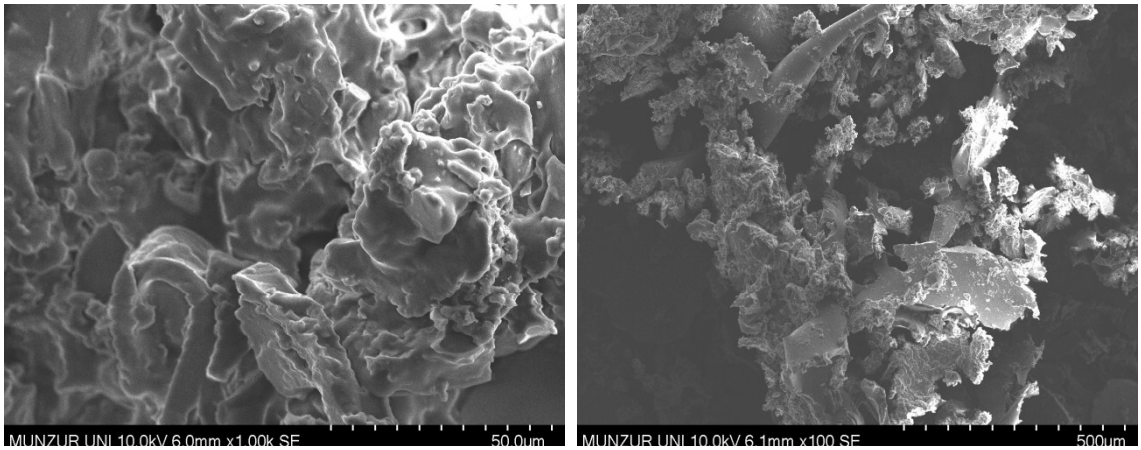

Figure 4.20: SEM image of cobalt nanoparticles synthesied by P.Harmala (EE) at different magnification levels.

The EDX profile (Table 4.6) shows a strong carbon signal along with weak silver as well as an oxygen peak, which may start due to the scorched of nanoparticles while drying. Also low inductive of Cl, Al, and Au were spotted (Figure 4.21a and b) showed a low amount of Ag with atomic composition of 50.71 %.

(a) (b)

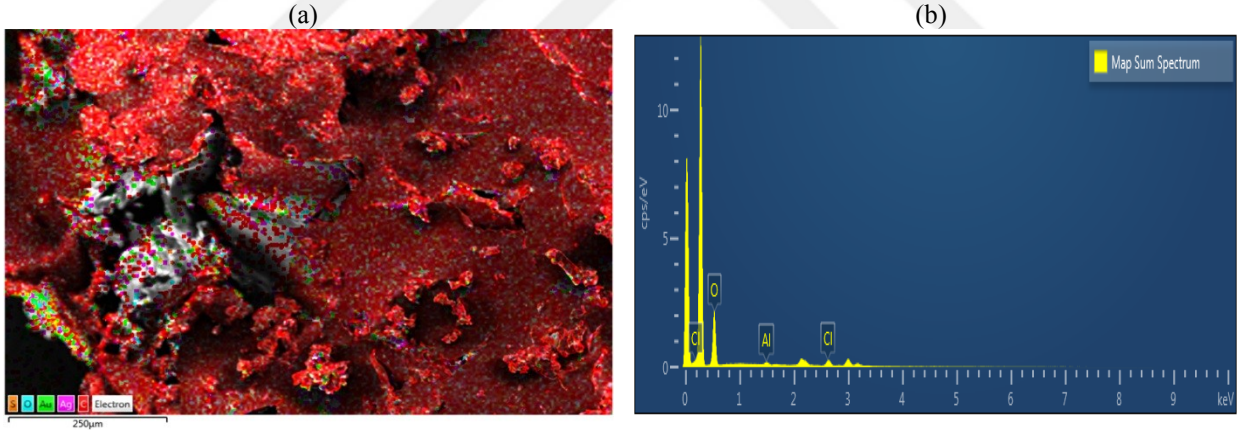

Figure 4.21: EDX spectrum of silver nanoparticles (a), division of silver element. (b), elemental mapping: electron micrograph area of AgNPs.

Table 4.6: EDX measurement of the atomic content in AgNPs synthesized at room temperature (EE).

Map Sum Spectrum				
Element	Line Type	Weight %	Weight % Sigma	Atomic %
C	K series	64.70	0.26	78.62
Ag	L series	7.60	0.19	1.03
Au	M series	4.68	0.20	0.35
Cl	K series	1.72	0.06	0.71
O	K series	20.93	0.19	19.09
Al	K series	0.38	0.03	0.20
Total		100		100

Elemental mapping analysis of cobalt nanoparticles synthesized by ethanol extract reveals a lower section of metallic cobalt in the image of cobalt nanoparticles scanned by electron micrograph (Figure 4.22a and b). The EDX analysis indicates a significant percentage of Co with an atomic structure of 35.37% from (Table 4.7). But the number of carbon atoms still higher than cobalt.

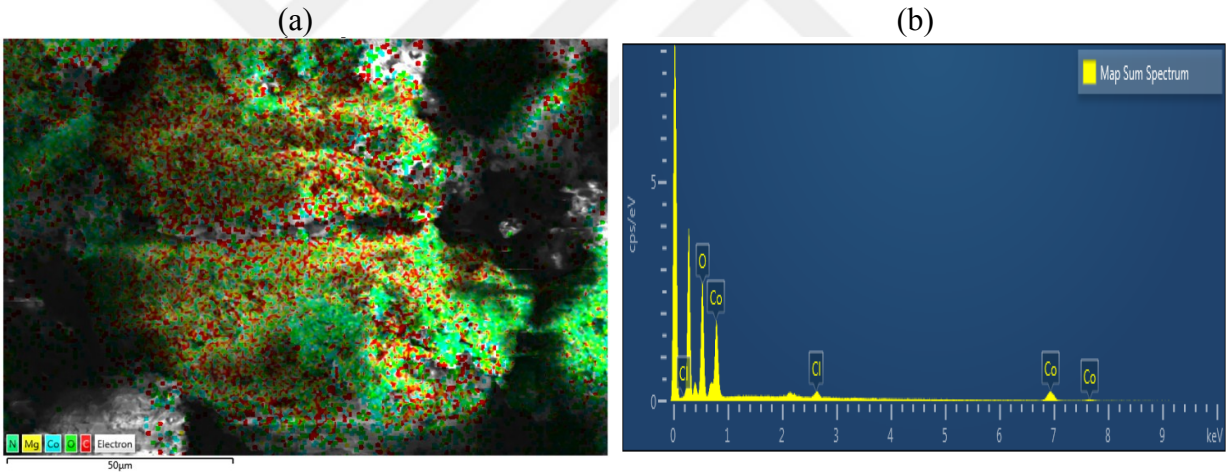

Figure 4.22: EDX spectrum of cbalt nanoparticles (a), distribution of cobalt element. (b), elemental mapping: electron micrograph region of cobalt nanoparticles.

Table 4.7: EDX measurement of the atomic content in CoNPs by P.Harmala seed at 25℃ (EE).

Map Sum Spectrum				
Element	Line Type	Weight %	Weight % Sigma	Atomic %
C	K series	38.51	0.44	60.75
O	K series	22.74	0.33	26.94
Co	L series	35.37	0.52	11.37
Cl	K series	1.40	0.10	0.75
Au	M series	1.98	0.36	0.19
Total		100		100

4.4.3. SEM and EDX analysis of Co, and Ag-CoNPs using methanol extract

In (Figure 4.23) the SEM picture indicates the morphological nature of the CoNPs produced by the methanol extract of P. Harmala at room temperature. The result showing the spherical shapes of nanoparticles.While (Figure 4.24) showed the morphological character for Ag-CoNPs, the SEM images of Ag-CoNPs showed cubic shapes.

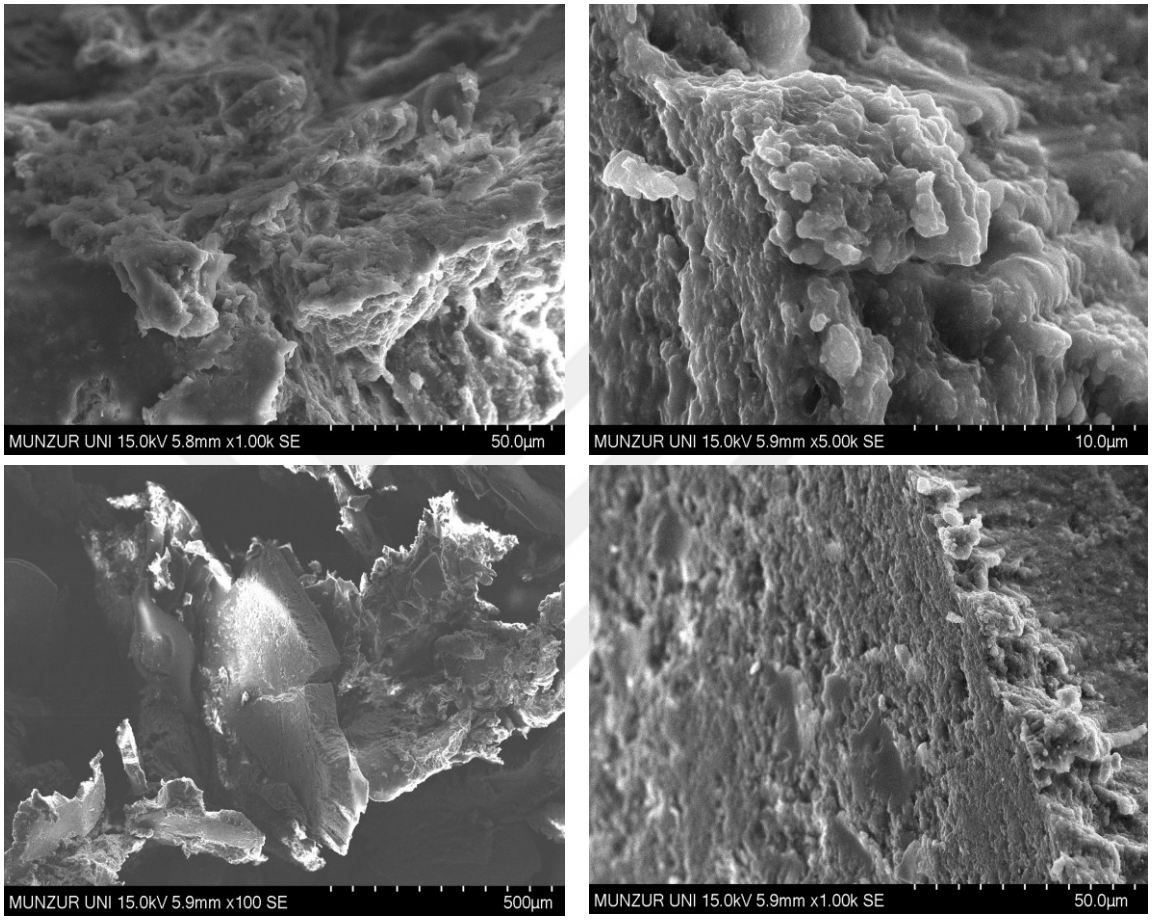

Figure 4.23: SEM image of cobalt nanoparticles synthesied by P.Harmala (ME) at various enlargement levels

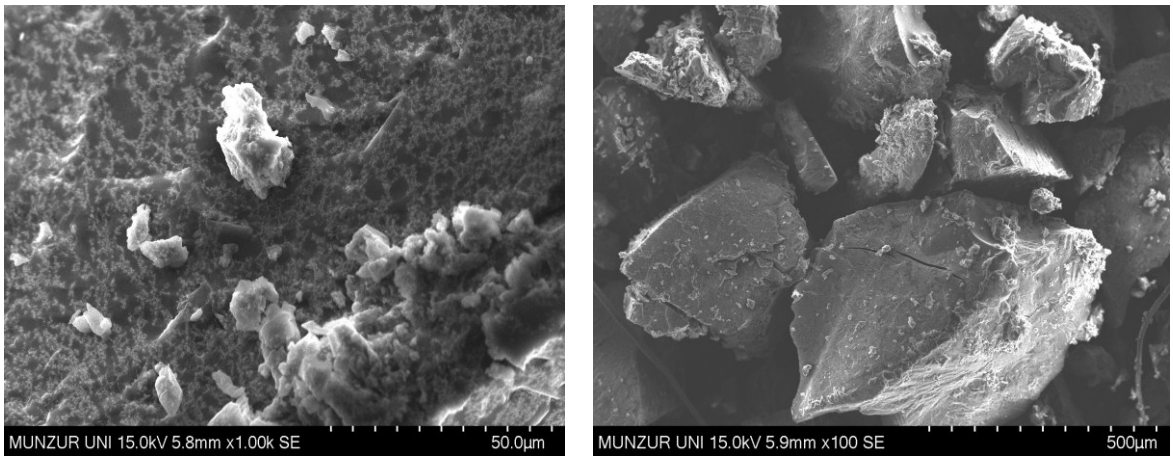

Figure 4.24: SEM image of silver-cobalt nanoparticles synthesied by P.Harmala (ME) at different magnification levels.

An analysis of the elemental mapping of cobalt nanoparticles synthesize by methanol extract reveals a division of minimum of cobalt atoms in the scanned electron micrograph picture of cobalt nanoparticles particles (Figure 4.25a and b). The EDX analysis indicate the amount of C atom elevated with atomic composition of 59.37 % of the synthesis Table 4.8 with the number of cobalt atoms 5.31%.

(a) (b)

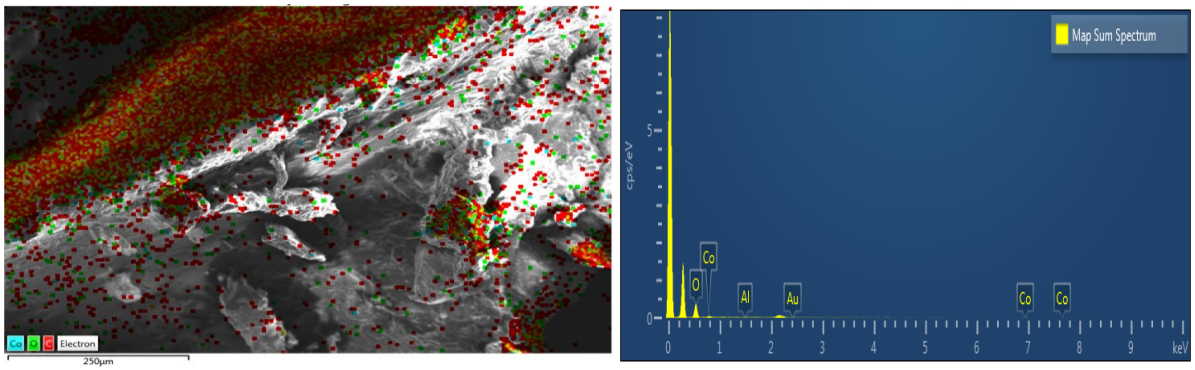

Figure 4.25: EDX spectrum of cobalt nanoparticles (a), distribution of cobalt element. (b), elemental mapping: electron micrograph region of cobalt nanoparticles.

Table 4.8: EDX measurement of the atomic content in CoNPs synthesized at room temperature (ME).

Map Sum Spectrum				
Element	Line Type	Weight %	Weight % Sigma	Atomic %
C	K series	59.55	0.73	74.39
O	K series	24.91	0.54	23.36
Au	M series	9.99	0.64	0.76
Co	L series	5.31	0.60	1.35
Al	K series	0.25	0.08	0.14
Total		100		100

The EDX profile, shows a strong carbon signal along with weak silver as well as a very weak signal of cobalt than oxygen peak, which may start due to the scorched of nanoparticles while drying. A tiny amount of spread of Cl and Au spotted. (Figure 4.26 a, and b) showed a low amount of Ag with an atomic composition of 20.15 %, with 0.36 % of cobalt nanoparticles.

(a) (b)

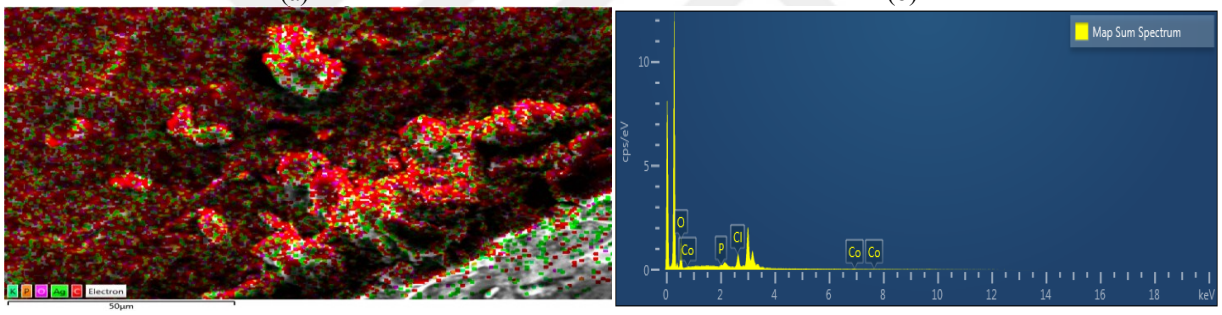

Figure 4.26: EDX spectrum of silver-cobalt nanoparticles (a), distribution of silver-cobalt element. (b), electron micrograph area of Ag-CoNPs.

Table 4.9: EDX measurement of the atomic content in Ag-CoNPs synthesized at 25℃ (ME).

Map Sum Spectrum				
Element	Line Type	Weight %	Weight % Sigma	Atomic %
C	K series	57.74	0.34	77.71
Ag	L series	20.15	0.25	3.02
Cl	K series	1.83	0.06	0.83
O	K series	17.90	0.30	18.08
Au	M series	1.82	0.20	0.15
P	K series	0.20	0.05	0.11
Co	K series	0.36	0.12	0.10
Total		100		100

4.5. **Antimicrobial activity of the Biosynthesized Nanoparticles**

In the present investigation, The antimicrobial affect studied through inhibitory activity of prepared Ag, Co, Ag-CoNPs on three different types of microorganism, utilizing the agar diffusion experiment on E. coli (Gram-negative), S. aureus (Gram-positive), and C. Albicans, are presented in Figure 4.27- 4.29. The result of the inhibition zone with the antibiotic control such as, Ceftriaxone, Dimethyl sulfoxide (DMSO), and for the yeast Nystatin are given in

Table 4.10, Table 4.11.

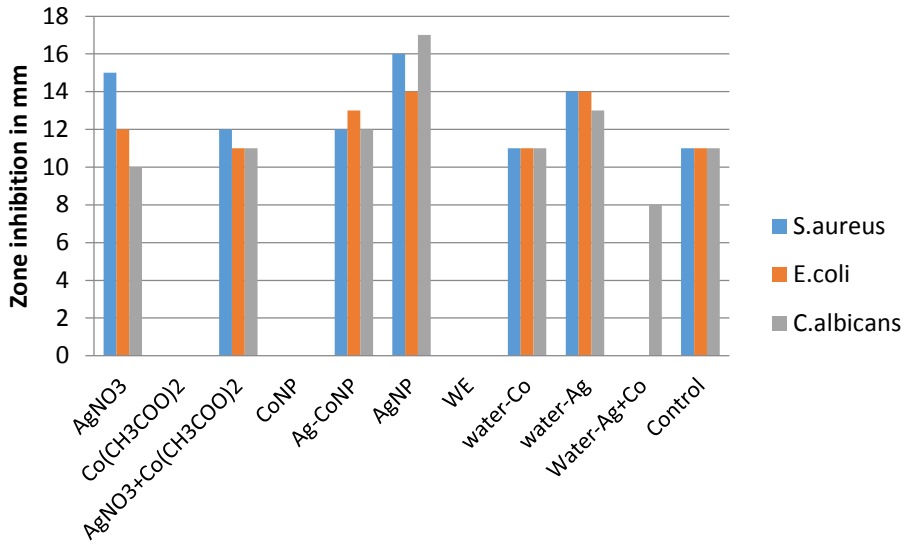

Figure 4.27: The figure shows the matchment of inhibition zones between, a) AgNPs, CoNPs, and bimetallic Ag-CoNPs synthesized using P. Harmala seed water extract, b) $AgNO_3$, $Co(CH_3COO)_2$, and $AgNO_3$+ $Co(CH_3COO)_2$ with water and water extract.

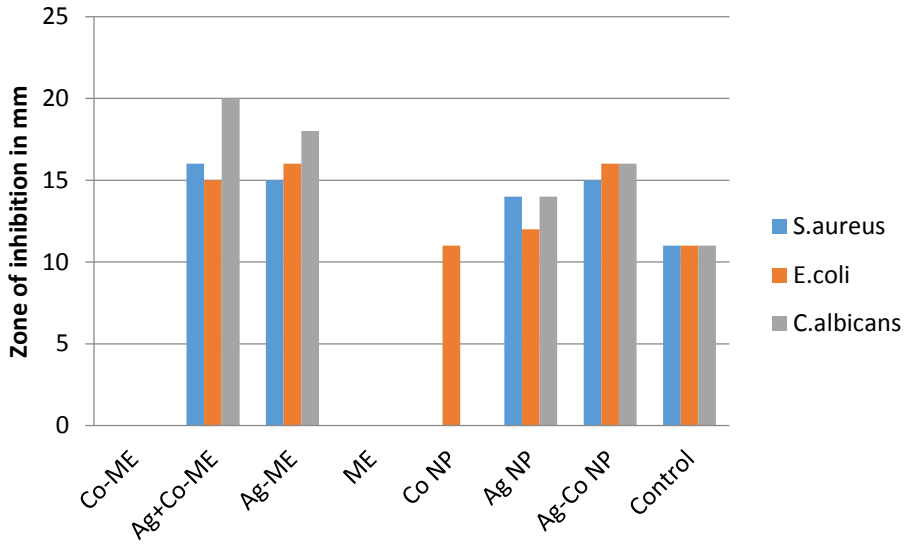

Figure 4.28: a) AgNPs, CoNPs, and Ag-CoNPs manufuctured by P. Harmala seed methanol extract, compared with b) $AgNO_3$, $Co(CH_3COO)_2$, and $AgNO_3$+ $Co(CH_3COO)_2$ with methanol extract. And controls.

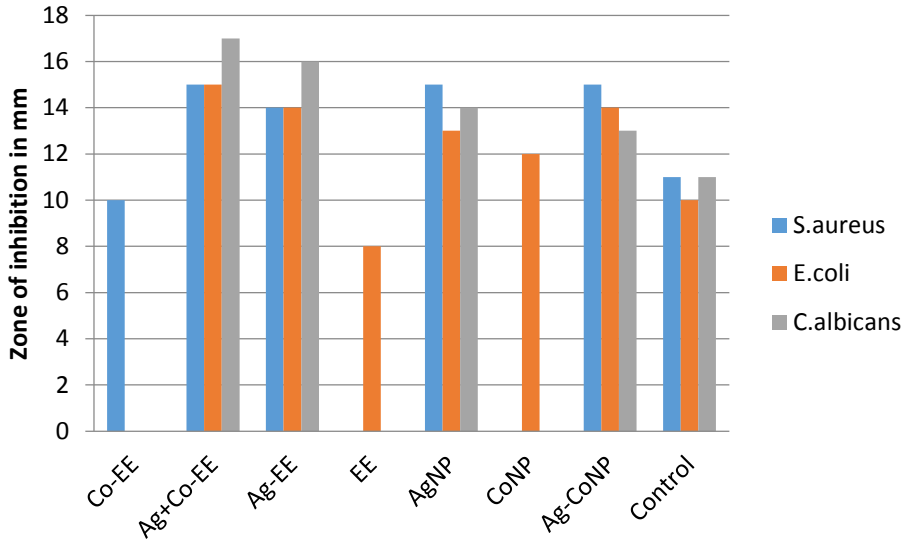

Figure 4.29: The figure clearifing the inhibition zones of, a) AgNPs, CoNPs, and Ag-CoNPs manugactured by P. Harmala seed ethanol extract, and compared with, b) $AgNO_3$, $Co(CH_3COO)_2$, and $AgNO_3$+ $Co(CH_3COO)_2$ with ethanol extract at room temperature.

Table 4.10: The 1-4 samples solutions, not nanoparticles, and; the others are solution contain plant extract.

	Name of sample	S.aureus	E.coli	C. albicans
1	$AgNO_3$ solution	15	12	10
2	$Co(CH_3COO)_2$ solution	-	-	-
3	$AgNO_3$+$Co(CH_3COO)_2$ solution	11	11	11
4	$Co(CH_3COO)_2$+WE	11	11	12
5	$AgNO_3$-$Co(CH_3COO)_2$+WE	-	-	8
6	$AgNO_3$ +WE	17	15	17
7	$Co(CH_3COO)_2$+ME	-	-	-
8	$AgNO_3$-$Co(CH_3COO)_2$+ME	16	15	20
9	$AgNO_3$ +ME	15	16	18
10	$Co(CH_3COO)_2$+EE	10	-	-
11	$AgNO_3$-$Co(CH_3COO)_2$+EE	15	15	17
12	$AgNO_3$ +EE	14	14	16
	Control	11	11	11

Table 4.11: Shows the inhibition zone of nanoparticle without plant extract, and with each plant extract.

	Name of sample	S.aureus	E.coli	C. albicans
1	Water Extract	-	-	-
2	CoNP (WE)	-	-	-
3	AgNP (WE)	14	12	13
4	Ag-CoNP (WE)	12	13	12
5	Metanol Extract	-	-	-
6	CoNP (ME)	-	11	-
7	AgNP (ME)	14	12	14
8	Ag-CoNP (ME)	15	16	16
9	Etanol Extract	-	8	-
10	CoNP (EE)	-	12	-
11	AgNP (EE)	15	13	14
12	Ag-CoNP (EE)	15	14	13
	Control	11	11	11

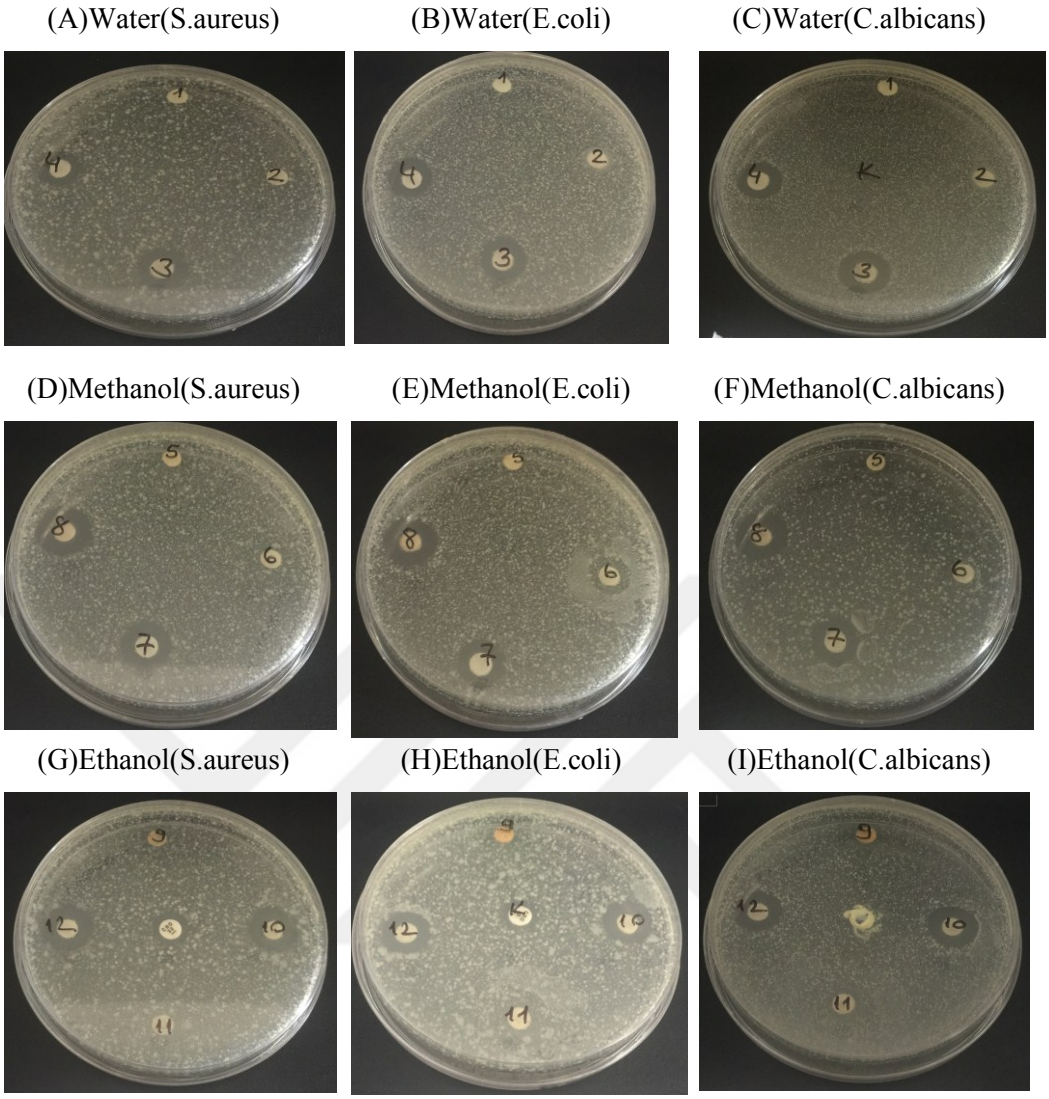

Figure 4.30: Antimicrobial activity of AgNPs, CoNPs, and Ag-CoNPs versus S.aureus, E.coli, and C.albicans using, A) Water, D) Methanol, and G) Ethanol extract of P.Harmala seed at room temperature.

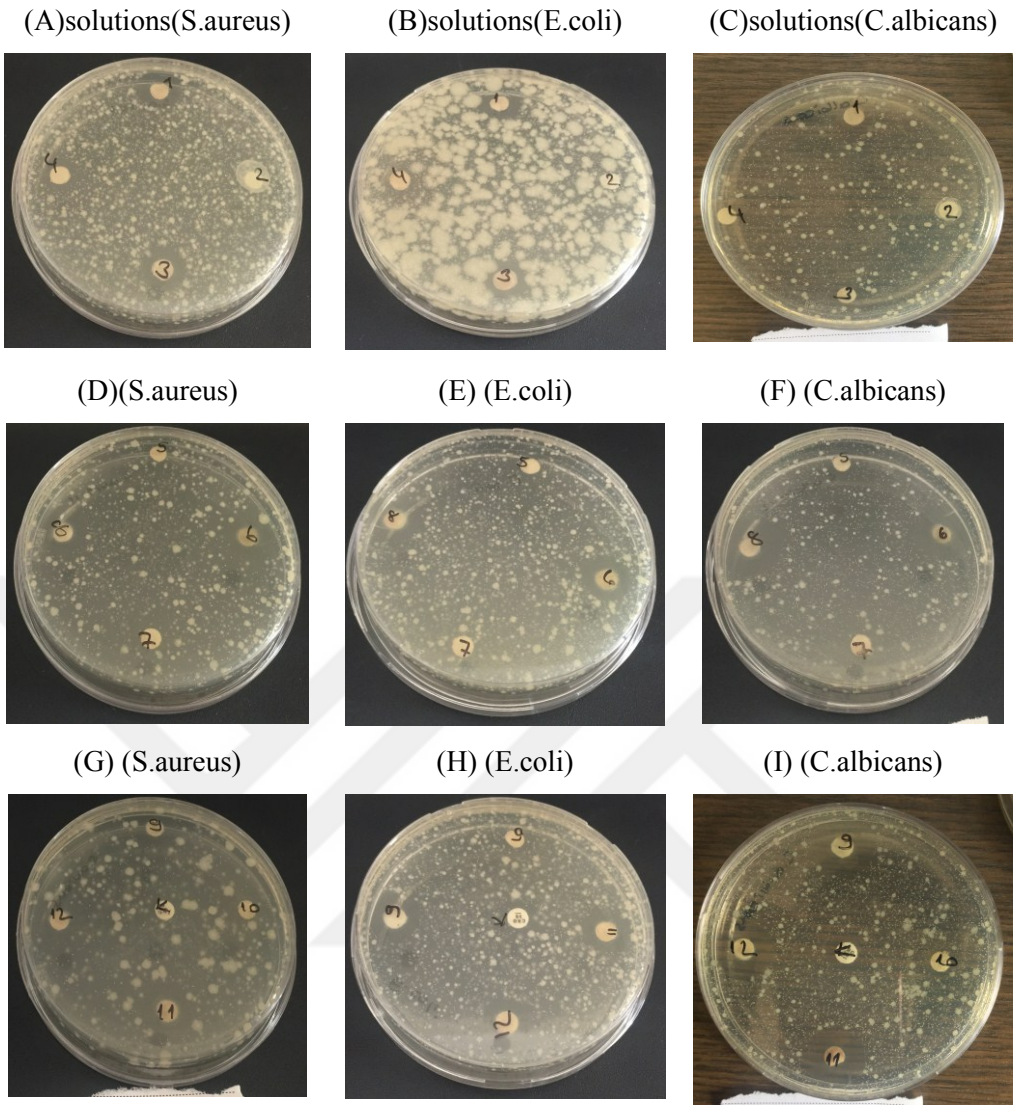

Figure 4.31: Antimicrobial activity of $AgNO_3$, $Co(CH_3COO)_2$, and $AgNO_3$+$Co(CH_3COO)_2$ solution versus S.aureus, E.coli, and C.albicans using A) Water, B) Methanol, and C) Ethanol extract, and each solution without extract.

From looking at the experimental discs, we find that the green synthetic nanoparticles showed an effect against the bacteria and fungi used. We also compared the effect of all nanoparticles separately according to the difference in the solvent used in the extraction, by measuring the size of the inhibition areas in millimeters (mm). Our results can be summarized as follows: Silver nanoparticles synthesized using water, ethanol, and methanol extract from P. seeds were observed to have activity recorded in three different plant extracts.

The area of inhibition against S. aureus for AgNPs was obtained as 14, 14, 15 mm, for Escherichia coli 12, 12, 13 mm, while for Albicans 13, 13, 14 mm, these results include a comparison of silver particles synthesized in three solvents. Used, as shown in (Figure 4.30 and

Table 4.10). The silver nanoparticles synthesized by ethanol extract showed better result against antibacterial and antifungal according to the zone inhibition.

However; the zone inhibition of Ag-CoNPs against S.aureus, E.coli, and C.albicans was obtained as (12, 15, 15 mm), (13, 16, 14 mm), and (12, 16, 13 mm) that synthesized by water, methanol, and ethanol respectively, according to the result Ag-CoNPs that synthesized by both methanol and ethanol extract showed high activity against present microorganisms. The zone inhibition in the

Table 4.10 showed no activity against the bacterial and fungal for synthesized CoNPs synthesized by water, methanol, and ethanol extract.

The silver nanoparticles, and silver-cobalt nanoparticles have resulted moderate antimicrobial activity compared to one inhibition diameter of control 11 mm. the result also observed that the $AgNO_3$, $AgNO_3$+$Co(CH_3COO)_2$ solution showed high activity against microorganism, which mixed with water, methanol, and ethanol extract, except $Co(CH_3COO)_2$ solution no activity was recorded in water, methanol, and ethanol extract.

In this study, AgNPs and Ag-CoNPs showed similar behavior towards inhibiting positive and negative bacteria. According to Al-Azizia et al., [65] they attributed the antimicrobial activity behavior of AgNPs to the attachment of silver ions to the cell wall of the microorganisms, and as a result of this attachment an interaction occurs between the cell membrane and the ions, which leads to plasmolysis and inhibition of the cell membrane, and more than this, The thiol group in bacterial proteins interacts with silver nanoparticles, and in turn stops DNA development and replication, by emission silver ions into the cell, causing respiratory chain reactions, cell division, and death.

5. CONCLUSIONS

Quick and easy synthesis of Ag monometallic particles, monometallic nanoparticles, and Ag-Co bimetallic particles by the method through the green plant by reducing $AgNO_3$ and Co $(NO_3)_2.6H_2O$ solutions. It was successfully achieved by returning. It is worth mentioning that the three solvents present in Peganum Harmala seeds used as extracts were examined in this study and showed a rapid and successful big improvement.

The formation of Ag, Co, Ag-CoNPs in three extracts was monitored by surface Plasmon resonance (λ max at 310-366 nm) and UV-vis spectra in all nanoparticles and without the use of heat. We first observed the formation of nanoparticles as early as one hour in the green synthesis which was carried out in the water extract and the reactions were completed within two hours for AgNPs in three extracts, but for Ag-CoNPs and CoNPs, it took more time. Ag, Co, Ag-CoNPs in both methanol and ethanol extract was very slowly and also the synthesis nanoparticles were adhesive and very difficult to handle and were not dissolved in any solution for the screening of UV spectra fully demonstrated rapid and successful bio reduction.

The XRD models confirmed the formation of Ag, Co, and Ag-Co bimetallic nanoparticles, due to their presenting peaks of their own. SEM analysis shows that the morphology of the AgNPs has a cubic shape; The Ag-CoNPs are also the same, while the CoNPs showed spherical shapes. The EDX spectrum emphasizes high silver signals in Ag NPs and Ag-Co NPs synthesized by water extract, the peak of cobalt was recorded for CoNPs synthesized by ethanol extract recorded strong peaks compared to water extract and methanol extract, the EDX spectrum was very weak in AgNPs synthesized by methanol extract. Due to our inability to dry the synthesized nanoparticles with ethanol extract and methanol, we encountered problems while analyzing the synthesized nanoparticles, which is why we do not have the data related to them.

The antimicrobial activity showed that the colloidal AgNPs and Ag-CoNPs synthesized by different P. Harmala seed extracts, inhibited and inhibited the growth of the test bacteria S.aureus, E.coli and C. by CoNPs in the three plant extracts.

The synthesized nanoparticles can be used by green synthesis methods for the manufacture of antibacterial drugs due to the bacterial activity of the Nano, as a result lays the manufacture of materials active against bacteria by free extracting green from medicinal plants. The particles must be free of impurities and dirt when it enters the manufacture of the therapeutic resource.

REFERENCES

[1] Aman Gour &Narendra Kumar Jain. (2019). Advances in Green Synthesis of Nanoparticles, Artificial Cells, Nanomedicine, and Biotechnology, 47:1, pp. 844-851, DOI: 10.1080/21691401.2019.1577878.

[2] Kesava Pandian S. (2010), Electrical, Optical and High Pressure Studies on some Transition Metals (Mn, Fe, Co, Ni, Cu, Zn) and Ce-DOPED SnO2 Nanoparticles, The Shodhganga@INFLIBNET, http://hdl.handle.net/10603/10662.

[3] Nath, Debjani, Banerjee, Pratyusha. (2013). Green Nanotechnology – A New Hope for Medical biology, Environmental Toxicology and Pharmacology, Vol. 36, ss. 3, pp. 997-1014. https://doi.org/10.1016/j.etap.2013.09.002.

[4] Wong TS, Schwaneberg U. (2003). Protein engineering in bioelectrocatalysis. Curr Opin Biotechnol, 14(6), ss. 590-6. doi: 10.1016/j.copbio.2003.09.008. PMID: 14662387.

[5] Makarov, V. V., Love, A. J., Sinitsyna, O. V., Makarova, S. S., Yaminsky, I. V., Taliansky, M. E., & Kalinina, N. O. (2014). "Green" nanotechnologies: synthesis of metal nanoparticles using plants. Acta naturae, 6(1), pp. 35–44.

[6] Tejaswi Thunugunta, Anand C, Reddy & Lakshmana Reddy. D. C. (2015). Green synthesis of nanoparticles: current prospectus, Nanotechnology Reviews 'Just Accepted' paper, ss. 2191-9097, DOI: 10.1515/ntrev-2015-0023.

[7] A. Anuoluwa Abimbola. (2017). Green Synthesis of Capped Silver Nanoparticles and Their Hybrids: Antimicrobial and Optical Properties, http://eprints.covenantuniversity.edu.ng/id/eprint/9513.

[8] Singh, J., Dutta, T., Kim, KH. et al. (2018). 'Green' synthesis of metals and their oxide nanoparticles: applications for environmental remediation. J Nanobiotechnol 16, 84. https://doi.org/10.1186/s12951-018-0408-4

[9] Mazur, M. (2004). Electrochemically prepared silver nanoflakes and nanowires. Electrochemistry Communications, 6(4), 400–403. doi:10.1016/j.elecom.2004.02.011.

[10] Di Guglielmo, C., López, D. R., De Lapuente, J., Mallafre, J. M. L., & Suàrez, M. B. (2010). Embryotoxicity of cobalt ferrite and gold nanoparticles: A first in vitro approach. Reproductive Toxicology, 30(2), 271–276. doi:10.1016/j.reprotox.2010.05.001.

[11] Creighton, J. A., Blatchford, C. G., & Albrecht, M. G. (1979). Plasma resonance enhancement of Raman scattering by pyridine adsorbed on silver or gold sol particles of size comparable to the excitation wavelength. Journal of the Chemical Society, Faraday Transactions 2, 75, 790. doi:10.1039/f29797500790.

[12] Shafey, A. M. E. (2020). Green synthesis of metal and metal oxide nanoparticles from plant leaf extracts and their applications: A review, Green Processing and Synthesis, 9(1), 304-339. doi: https://doi.org/10.1515/gps-2020-0031.

[13] Evanoff, D. D. & Chumanov-Jr., G. (2003). Size-controlled synthesis of nanoparticles measurement of extinction, scattering and absorption cross sections. Journal of Physical Chemistry B, 108, 13957-13962. https://doi.org/10.1021/jp047565s.

[14] Jinous Asgarpanah and Fereshteh Ramezanloo. (2012). Chemistry, pharmacology and medicinal properties of Peganum harmala L., African Journal of Pharmacy and Pharmacology, 6(22), pp. 1573-1580, ss. 1996-0816. DOI: 10.5897/AJPP11.876. http://www.academicjournals.org/AJPP.

[15] Suzuki, K., Nomura, I., Ninomiya, M., Tanaka, K., & Koketsu, M. (2018). Synthesis and antimicrobial activity of β-carboline derivatives with N2-alkyl modifications. Bioorganic & Medicinal Chemistry Letters, 28(17), 2976–2978. doi:10.1016/j.bmcl.2018.06.050.

[16] Iranshahy M, Fazly Bazzaz S, Haririzadeh G, Abootorabi BZ, Mohamadi AM, Khashyarmanesh Z. (2019). Chemical composition and antibacterial properties of Peganum harmala L. Avicenna J Phytomed, 9(6): 530-537. DOI: 10.22038/AJP.2019.13382.

[17] Gurunathan, S., Park, J. H., Han, J. W., & Kim, J.-H. (2015). Comparative assessment of the apoptotic potential of silver nanoparticles synthesized by Bacillus tequilensis and Calocybe indica in MDA-MB-231 human breast cancer cells: targeting p53 for anticancer therapy. International Journal of Nanomedicine, 4203. doi:10.2147/ijn.s83953.

[18] Pirtarighat, S., Ghannadnia, M. & Baghshahi, S. (2019). Green synthesis of silver nanoparticles using the plant extract of Salvia spinosa grown in vitro and their antibacterial activity assessment. J Nanostruct Chem 9, 1–9. https://doi.org/10.1007/s40097-018-0291-4.

[19] Ansari, S. M., Bhor, R. D., Pai, K. R., Sen, D., Mazumder, S., Ghosh, K., … Ramana, C. V. (2017). Cobalt nanoparticles for biomedical applications: Facile synthesis, physiochemical characterization, cytotoxicity behavior and biocompatibility. Applied Surface Science, 414, 171–187. doi:10.1016/j.apsusc.2017.03.002.

[20] Kashif Ahmed, Iqbal Tariq, Solat Ullah Siddiqui and Muhammad Mudassir. (2016). Green synthesis of cobalt nanoparticles by using methanol extract of plant leaf as reducing agent, . Pure and Applied Biology, 5(3), pp. 453-457. http://dx.doi.org/10.19045/bspab.2016.50058.

[21] Rama Koyyati, Karunakar Rao Kudle and Pratap Rudra Manthur Padigya. (2016). Evaluation of Antibacterial and Cytotoxic activity of Green Synthesized Cobalt Nanoparticles using Raphanus sativus var. longipinnatus Leaf Extract, International Journal of PharmTech ResearCH, 9(3), ss. 0974-4304 , pp 466-472.

[22] Saba Naz, Abdul Rauf Khaskheli, Abdalaziz Aljabour, Huseyin Kara, Farah Naz Talpur, Syed Tufail Hussain Sherazi, Abid Ali Khaskheli, Sana Jawaid, (2014). "Synthesis of Highly Stable Cobalt Nanomaterial Using Gallic Acid and Its Application in Catalysis", Advances in Chemistry, vol. 2014, Article ID 686925, 6 pages. https://doi.org/10.1155/2014/686925.

[23] Al-Haddad, J., Alzaabi, F., Pal, P. et al. (2020). Green synthesis of bimetallic copper–silver nanoparticles and their application in catalytic and antibacterial activities. Clean Techn Environ Policy, 22, pp.269–277. https://doi.org/10.1007/s10098-019-01765-2.

[24] Tooba Mazhar, Vikas Shrivastava and Rajesh Singh Tomar. (2017). Green Synthesis of Bimetallic Nanoparticles and its Applications: A Review, J. Pharm. Sci. & Res., 9(2), pp. 102-110.

[25] Kanwal Z, Raza MA, Riaz S, Manzoor S, Tayyeb A, Sajid I, Naseem S. (2019). Synthesis and characterization of silver nanoparticle-decorated cobalt nanocomposites (Co@AgNPs) and their density-dependent antibacterial activity, R. Soc. open sci. 6: 182135. http://dx.doi.org/10.1098/rsos.182135.

[26] Gurunathan, S., Raman, J., Abd Malek, S. N., John, P. A., & Vikineswary, S. (2013). Green synthesis of silver nanoparticles using Ganoderma neo-japonicum Imazeki: a potential cytotoxic agent against breast cancer cells. International journal of nanomedicine, 8, 4399–4413. https://doi.org/10.2147/IJN.S51881.

[27] Ju-Nam, Y., & Lead, J. R. (2008). Manufactured nanoparticles: An overview of their chemistry, interactions and potential environmental implications. Science of The Total Environment, 400(1-3), 396–414. doi:10.1016/j.scitotenv.2008.06.042.

[28] Liu, J., Sutton, J., & Roberts, C. B. (2007). Synthesis and Extraction of Monodisperse Sodium Carboxymethylcellulose-Stabilized Platinum Nanoparticles for the Self-assembly of Ordered Arrays. The Journal of Physical Chemistry C, 111(31), 11566–11576. doi:10.1021/jp071967t.

[29] Herrera, A. P., Resto, O., Briano, J. G., & Rinaldi, C. (2005). Synthesis and agglomeration of gold nanoparticles in reverse micelles. Nanotechnology, 16(7), S618–S625. doi:10.1088/0957-4484/16/7/040.

[30] Iravani, S. (2011). Green synthesis of metal nanoparticles using plants. Green Chemistry, 13(10), 2638. doi:10.1039/c1gc15386b.

[31] Wu, M.-L., Chen, D.-H., & Huang, T.-C. (2001). Preparation of Au/Pt Bimetallic Nanoparticles in Water-in-Oil Microemulsions. Chemistry of Materials, 13(2), 599–606. doi:10.1021/cm0006502.

[32] Boca, S. C., & Astilean, S. (2010). Detoxification of gold nanorods by conjugation with thiolated poly(ethylene glycol) and their assessment as SERS-active carriers of Raman tags. Nanotechnology, 21(23), 235601. doi:10.1088/0957-4484/21/23/235601.

[33] Parveen, K., Banse, V., & Ledwani, L. (2016). Green synthesis of nanoparticles: Their advantages and disadvantages. doi:10.1063/1.4945168.

[34] Feynman, Richard P. (1960) There's Plenty of Room at the Bottom. Engineering and Science, 23 (5). pp. 22-36, ss. 0013-7812. https://resolver.caltech.edu/CaltechES:23.5.1960Bottom..

[35] Antariksh Saxena, R.M. Tripathi, R. P. Singh. (2010). Biological synthesis of silver nanoparticles by using onion (allium cepa) extract and their antibacterial activity, Digest Journal of Nanomaterials and Biostructures Vol. 5, No 2, p. 427 – 432.

[36] Happy Agarwal, S. Venkat Kumar, S. Rajeshkumar. (2017). “A review on green synthesis of zinc oxide nanoparticles –An eco-friendly approach” Resource-Efficient Technologies, pp. 406–413. http://creativecommons.org/licenses/by-nc-nd/4.0/.

[37] Iqbal, P., Preece, J. A., & Mendes, P. M. (2012). Nanotechnology: The “Top-Down” and “Bottom-Up” Approaches. Supramolecular Chemistry. doi:10.1002/9780470661345.smc195.

[38] Wubshet Belay Abagero. (2017). Exploring the potentialities of waste plant materials for the production of gold nanoparticles and multi-metallic composite particles and its application in wastewater treatment, Universidade do Algarve. http://hdl.handle.net/10400.1/10135.

[39] Mohanpuri P, Rana NK, Yadav SK. (2008). Biosynthesis of nanoparticles, technological concepts and future applications. J Nanopart Res., 10, 507–517. DOI 10.1007/s11051-007-9275-x.

[40] Mohanpuria, P., Rana, N.K. & Yadav, S.K. (2008). Biosynthesis of nanoparticles: technological concepts and future applications. J Nanopart Res 10, 507–517. https://doi.org/10.1007/s11051-007-9275-x

[41] Rauwel, P., Küünal, S., Ferdov, S., & Rauwel, E. (2015). A Review on the Green Synthesis of Silver Nanoparticles and Their Morphologies Studied via TEM. Advances in Materials Science and Engineering, 2015, 1–9. doi:10.1155/2015/682749.

[42] Husseiny, M. I., El-Aziz, M. A., Badr, Y., & Mahmoud, M. A. (2007). Biosynthesis of gold nanoparticles using Pseudomonas aeruginosa. Spectrochimica Acta Part A: Molecular and Biomolecular Spectroscopy, 67(3-4), 1003–1006. doi:10.1016/j.saa.2006.09.028.

[43] Singh, P., Kim, Y.-J., Zhang, D., & Yang, D.-C. (2016). Biological Synthesis of Nanoparticles from Plants and Microorganisms. Trends in Biotechnology, 34(7), 588–599. doi:10.1016/j.tibtech.2016.02.006.

[44] Manish Soni, Priya Mehta, Anjali Soni And Girish K. Goswami. (2018). Green Nanoparticles: Synthesis and Applications, IOSR Journal of Biotechnology and Biochemistry (IOSR-JBB), 4(3), pp. 78-83, ss. 2455-264X, DOI: 10.9790/264X-0403017883.

[45] Mukherjee, P., Ahmad, A., Mandal, D., Senapati, S., Sainkar, S. R., Khan, M. I., Kumar, R. (2001). Bioreduction of AuCl4− Ions by the Fungus, Verticillium sp. and Surface Trapping of the Gold Nanoparticles Formed D.M. and S.S. thank the Council of Scientific and Industrial Research (CSIR), Government of India, for financial assistance. Angewandte Chemie International Edition, 40(19), 3585. doi:10.1002/1521-3773(20011001)40:19<3585::aid-anie3585>3.0.co;2-k .

[46] Iravani, S. (2014). Bacteria in Nanoparticle Synthesis: Current Status and Future Prospects. International Scholarly Research Notices, 2014, 1–18. doi:10.1155/2014/359316.

[47] Klaus, T., Joerger, R. Olsson, E. & Granqvist, C. G. (1999). Silver based crystalline nanoparticles, microbially fabricated. Proceedings of the National Academy of Sciences of the United States of America, 96 (24), 13611–13614.; https://doi.org/10.1073/pnas.96.24.13611.

[48] Samadi, N., Golkaran, D., Eslamifar, A., Jamalifar, H., Fazeli, M. R., & Mohseni, F. A. (2009). Intra/Extracellular Biosynthesis of Silver Nanoparticles by an Autochthonous Strain of Proteus mirabilis Isolated fromPhotographic Waste. Journal of Biomedical Nanotechnology, 5(3), 247–253. doi:10.1166/jbn.2009.1029.

[49] Morley, G. F., & Gadd, G. M. (1995). Sorption of toxic metals by fungi and clay minerals. Mycological Research, 99(12), 1429–1438. doi:10.1016/s0953-7562(09)80789-2.

[50] Saifuddin, N., Wong, C. W., & Yasumira, A. A. N. (2009). Rapid Biosynthesis of Silver Nanoparticles Using Culture Supernatant of Bacteria with Microwave Irradiation. E-Journal of Chemistry, 6(1), 61–70. doi:10.1155/2009/734264.

[51] Kalimuthu, K., Suresh Babu, R., Venkataraman, D., Bilal, M., & Gurunathan, S. (2008). Biosynthesis of silver nanocrystals by Bacillus licheniformis. Colloids and Surfaces B: Biointerfaces, 65(1), 150–153. doi:10.1016/j.colsurfb.2008.02.018.

[52] Nair, B., & Pradeep, T. (2002). Coalescence of Nanoclusters and Formation of Submicron Crystallites Assisted byLactobacillusStrains. Crystal Growth & Design, 2(4), 293–298. doi:10.1021/cg0255164.

[53] Ahmad, N., Sharma, S., Singh, V. N., Shamsi, S. F., Fatma, A., & Mehta, B. R. (2011). Biosynthesis of Silver Nanoparticles from Desmodium triflorum: A Novel Approach Towards Weed Utilization. Biotechnology Research International, 2011, 1–8. doi:10.4061/2011/454090.

[54] Durán, N., Marcato, P. D., Alves, O. L., De Souza, G. I., & Esposito, E. (2005). Journal of Nanobiotechnology, 3(1), 8. doi:10.1186/1477-3155-3-8.

[55] Balaji, D. S., Basavaraja, S., Deshpande, R., Mahesh, D. B., Prabhakar, B. K., & Venkataraman, A. (2009). Extracellular biosynthesis of functionalized silver nanoparticles by strains of Cladosporium cladosporioides fungus. Colloids and Surfaces B: Biointerfaces, 68(1), 88–92. doi:10.1016/j.colsurfb.2008.09.022.

[56] Mandal, D., Bolander, M. E., Mukhopadhyay, D., Sarkar, G., & Mukherjee, P. (2005). The use of microorganisms for the formation of metal nanoparticles and their application. Applied Microbiology and Biotechnology, 69(5), 485–492. doi:10.1007/s00253-005-0179-3.

[57] Mourato, A., Gadanho, M., Lino, A. R. and Tenreiro, R. (2011). Biosynthesis of crystalline silver and gold nanoparticles by extremophilic yeasts. Bioinorganic Chemistry and Applications. Vol. 2011, Article ID 546074, 8 pages. Doi:10.1155/2011/546074.

[58] Apte, M., Sambre, D., Gaikawad, S., Joshi, S., Bankar, A., Kumar, A. R., & Zinjarde, S. (2013). Psychrotrophic yeast Yarrowia lipolytica NCYC 789 mediates the synthesis of antimicrobial silver nanoparticles via cell-associated melanin. AMB Express, 3(1), 32. https://doi.org/10.1186/2191-0855-3-32.

[59] Singaravelu, G., Arockiamary, J. S., Kumar, V. G., & Govindaraju, K. (2007). A novel extracellular synthesis of monodisperse gold nanoparticles using marine alga, Sargassum wightii Greville. Colloids and Surfaces B: Biointerfaces, 57(1), 97–101. doi:10.1016/j.colsurfb.2007.01.010.

[60] Shakeel Ahmed, Mudasir Ahmad, Babu Lal Swami, Saiqa Ikram . (2016). A review on plants extract mediated synthesis of silver nanoparticles for antimicrobial applications: A green expertise, Journal of Advanced Research , 7, 17–28. http://dx.doi.org/10.1016/j.jare.2015.02.007.

[61] Leela A, Vivekanandan M. (2008). Tapping the unexploited plant resources for the synthesis of silver nanoparticles. African J of Biotechnology, 7 (17), pp. 3162-3165. http://www.academicjournals.org/AJB.

[62] Dhuper S, Panda D, Nayak PL. (2012). Green synthesis and characterization of zero valent iron nanoparticles from the leaf extract of Mangifera indica. Nano Trends: J Nanotech App, 13(2):16–22.

[63] Haradhan Kolya, Parthapratim Maiti, Akhil Pandey & Tridib Tripathy. (2015). Green synthesis of silver nanoparticles with antimicrobial and azo dye (Congo red) degradation properties using Amaranthus gangeticus Linn leaf extract, Journal of Analytical Science and Technology, 6:33, DOI 10.1186/s40543-015-0074-1.

[64] Mehdi Fazlzadeha, Rasoul Khosravi, Ahmad Zarei. (2017). Green synthesis of zinc oxide nanoparticles using Peganum harmala seed extract, and loaded on Peganum harmala seed powdered activated carbon as new adsorbent for removal of Cr(VI) from aqueous solution, Ecological Engineering, 103, pp. 180-190. https://doi.org/10.1016/j.ecoleng.2017.02.052.

[65] Matin Azizi, Sajjad Sedaghat, Kambiz Tahvildari, Pirouz Derakhshi & Ahad Ghaemi (2017) Synthesis of silver nanoparticles using Peganum harmala extract as a green route, Green Chemistry Letters and Reviews, 10:4, 420-427, DOI: 10.1080/17518253.2017.1395081.

[66] Nur Oktri Mulya Dewi, Yoki Yulizar, Dewangga Oky Bagus Apriandanu. (2019). Green synthesis of Co3O4 nanoparticles using Euphorbia heterophylla L. leaves extract: characterization and photocatalytic activity, IOP Conf. Series: Materials Science and Engineering, 509 ,012105. doi:10.1088/1757-899X/509/1/012105.

[67] Akinsiku, A. A., Dare, E. O., Ajanaku, K. O., Ajani, O. O., Olugbuyiro, J. A. O., Siyanbola, T. O., Emetere, M. E. (2018). Modeling and Synthesis of Ag and Ag/Ni Allied Bimetallic Nanoparticles by Green Method: Optical and Biological Properties. International Journal of Biomaterials, 2018, 1–17. doi:10.1155/2018/9658080.

[68] Juan Carlos Martínez Espinosa, Raúl Carrera Cerritos, Maria Antonieta Ramírez Morales, Karla Paola Sánchez Guerrero, Rocio Alejandra Silva Contreras and Juan H. Macías. (2020). Characterization of Silver Nanoparticles Obtained by a Green Route and Their Evaluation in the Bacterium of Pseudomonas aeruginosa, crystals MDPI, 10, 395; doi:10.3390/cryst10050395.

[69] Siddhant Jain & Mohan Singh Mehata. (2017). Medicinal Plant Leaf Extract and Pure Flavonoid Mediated Green Synthesis of Silver Nanoparticles and their Enhanced Antibacterial Property, ScienTific REPORTS, 7 (15867). DOI:10.1038/s41598-017 15724-8.

[70] Peter Logeswari, Sivagnanam Silambarasan, Jayanthi Abraham. (2012). Synthesis of silver nanoparticles using plants extract and analysis of their antimicrobial property, Journal of Saudi Chemical Society. http://dx.doi.org/10.1016/j.jscs.2012.04.007.

[71] Rodríguez-Luis, O. E., Hernandez-Delgadillo, R., Sánchez-Nájera, R. I., Martínez-Castañón, G. A., Niño-Martínez, N., Sánchez Navarro, M. del C., Cabral-Romero, C. (2016). Green Synthesis of Silver Nanoparticles and Their Bactericidal and Antimycotic Activities against Oral Microbes. Journal of Nanomaterials, 2016, 1–10. doi:10.1155/2016/9204573.

[72] Bilal Haider Abbasi, Mehreen Zaka, Syed Salman Hashmi, Zeeshan Khan. (2018). Biogenic synthesis of Au, Ag and Au–Ag alloy nanoparticles using Cannabis sativa leaf extract, IET Nanobiotechnology, 12(3), pp. 277 – 284. DOI: 10.1049/iet-nbt.2017.0169.

[73] Aliyaa A. Urabe and Wisam J. Aziz. (2019). Biosynthesis of cobalt oxide (Co3O4) nanoparticles using plant extract of Camellia sinensis (L.) Kuntze and Apium graveolens L. as the antibacterial application, World News of Natural Sciences, 24, pp. 357-365. www.worldnewsnaturalsciences.com.

[74] V. Subha, S. Kirubanandan, S. Renganathan. (2017). Green Synthesis of Copper Nanoparticles Using Methanol Extract of Passiflora foetida and Its Drug Delivery Applications, International Journal of Green Chemistry, 3(2), pp. 31–52.

[75] Mendes, R., Garbeva, P., & Raaijmakers, J. M. (2013). The rhizosphere microbiome: significance of plant beneficial, plant pathogenic, and human pathogenic microorganisms. FEMS Microbiology Reviews, 37(5), 634–663. doi:10.1111/1574-6976.12028.

[76] Cohen, T., & Murray, M. (2004). Modeling epidemics of multidrug-resistant M. tuberculosis of heterogeneous fitness. Nature medicine, 10(10), 1117–1121. https://doi.org/10.1038/nm1110.

[77] Scheffer, R.P. (1991). Role of toxins in evolution and ecology of plant pathogenic fungi. Experientia 47, 804–811. https://doi.org/10.1007/BF01922460.

[78] Lynch, M., & Conery, J. S. (2003). The Origins of Genome Complexity. Science, 302(5649), 1401–1404. doi:10.1126/science.1089370.

[79] Hahn, H. P. (1997). The type-4 pilus is the major virulence-associated adhesin of Pseudomonas aeruginosa – a review. Gene, 192(1), 99–108. doi:10.1016/s0378-1119(97)00116-9.

[80] Isberg, R. R., Voorhis, D. L., & Falkow, S. (1987). Identification of invasin: A protein that allows enteric bacteria to penetrate cultured mammalian cells. Cell, 50(5), 769–778. doi:10.1016/0092-8674(87)90335-7.

[81] Tsarfaty, H. Sandovsky-Losica, Leonid Mittelman , I. Berdicevsky, E. Segal. (2000). Cellular actin is a¡ected by interaction with Candida albicans, FEMS Microbiology Letters, 189, 225-232.

[82] Masalha, M., Borovok, I., Schreiber, R., Aharonowitz, Y., & Cohen, G. (2001). Analysis of transcription of the Staphylococcus aureus aerobic class Ib and anaerobic class III ribonucleotide reductase genes in response to oxygen. Journal of bacteriology, 183(24), 7260–7272. https://doi.org/10.1128/JB.183.24.7260-7272.2001.

[83] Gnanamani, A., Hariharan, P., & Paul-Satyaseela, M. (2017). Staphylococcus aureus: Overview of Bacteriology, Clinical Diseases, Epidemiology, Antibiotic Resistance and Therapeutic Approach. Frontiers in Staphylococcus Aureus. doi:10.5772/67338.

[84] GOULD, D., & CHAMBERLAINE, A. (1995). Staphylococcus aureus: a review of the literature. Journal of Clinical Nursing, 4(1), 5–12. doi:10.1111/j.1365-2702.1995.tb00004.x.

[85] Liu, G. Y., Essex, A., Buchanan, J. T., Datta, V., Hoffman, H. M., Bastian, J. F., Nizet, V. (2005). Staphylococcus aureusgolden pigment impairs neutrophil killing and promotes virulence through its antioxidant activity. The Journal of Experimental Medicine, 202(2), 209–215. doi:10.1084/jem.20050846.

[86] Blair, J. E. (1958). Factors Determining the Pathogenicity of Staphylococci. Annual Review of Microbiology, 12(1), 491–506. doi:10.1146/annurev.mi.12.100158.002423.

[87] Brown, D. F. J., Edwards, D. I., Hawkey, P. M., Morrison, D., Ridgway, G. L., Towner, K. J., & Wren, M. W. D. (2005). Guidelines for the laboratory diagnosis and susceptibility testing of methicillin-resistant Staphylococcus aureus (MRSA). Journal of Antimicrobial Chemotherapy, 56(6), 1000–1018. doi:10.1093/jac/dki372.

[88] Lindsay, J. A., & Holden, M. T. G. (2004). Staphylococcus aureus : superbug, super genome? Trends in Microbiology, 12(8), 378–385. doi:10.1016/j.tim.2004.06.004.

[89] Schlecht, L. M., Peters, B. M., Krom, B. P., Freiberg, J. A., Hänsch, G. M., Filler, S. G., Jabra-Rizk, M. A., & Shirtliff, M. E. (2015). Systemic Staphylococcus aureus infection mediated by Candida albicans hyphal invasion of mucosal tissue. Microbiology (Reading, England), 161(Pt 1), 168–181. https://doi.org/10.1099/mic.0.083485-0.

[90] Diekema, D. J., Pfaller, M. A., Schmitz, F. J., Smayevsky, J., Bell, J., Jones, R. N. (2001). Survey of Infections Due toStaphylococcusSpecies: Frequency of Occurrence and Antimicrobial Susceptibility of Isolates Collected in the United States, Canada, Latin America, Europe, and the Western Pacific Region for the SENTRY Antimicrobial Surveillance Program, 1997–1999. Clinical Infectious Diseases, 32(s2), S114–S132. doi:10.1086/320184 .

[91] Lowy, F. D. (1998). Staphylococcus aureusInfections. New England Journal of Medicine, 339(8), 520–532. doi:10.1056/nejm199808203390806.

[92] KANEKO, J., & KAMIO, Y. (2004). Bacterial Two-component and Hetero-heptameric Pore-forming Cytolytic Toxins: Structures, Pore-forming Mechanism, and Organization of the Genes. Bioscience, Biotechnology, and Biochemistry, 68(5), 981–1003. doi:10.1271/bbb.68.981.

[93] Speziale, P., Pietrocola, G., Rindi, S., Provenzano, M., Provenza, G., Di Poto, A., Arciola, C. R. (2009). Structural and functional role ofStaphylococcus aureussurface components recognizing adhesive matrix molecules of the host. Future Microbiology, 4(10), 1337–1352. doi:10.2217/fmb.09.102.

[94] Kaper, J., Nataro, J. & Mobley, H. (2004). Pathogenic Escherichia coli. Nat Rev Microbiol 2, 123–140. https://doi.org/10.1038/nrmicro818.

[95] Croxen, M., Finlay, B. (2010). Molecular mechanisms of Escherichia coli pathogenicity. Nat Rev Microbiol 8, 26–38. https://doi.org/10.1038/nrmicro2265.

[96] Croxen, M. A., Law, R. J., Scholz, R., Keeney, K. M., Wlodarska, M., & Finlay, B. B. (2013). Recent Advances in Understanding Enteric Pathogenic Escherichia coli. Clinical Microbiology Reviews, 26(4), 822–880. doi:10.1128/cmr.00022-13.

[97] Hooper, L. V. (2001). Commensal Host-Bacterial Relationships in the Gut. Science, 292(5519), 1115–1118. doi:10.1126/science.1058709.

[98] Meiller, T. F., Hube, B., Schild, L., Shirtliff, M. E., Scheper, M. A., Winkler, R., Jabra-Rizk, M. A. (2009). A Novel Immune Evasion Strategy of Candida albicans: Proteolytic Cleavage of a Salivary Antimicrobial Peptide. PLoS ONE, 4(4), e5039. doi:10.1371/journal.pone.0005039.

[99] Sobel, J. D. (1997). Vaginitis. New England Journal of Medicine, 337(26), 1896–1903. doi:10.1056/nejm199712253372607.

[100] Pfaller, M. A., & Diekema, D. J. (2007). Epidemiology of Invasive Candidiasis: a Persistent Public Health Problem. Clinical Microbiology Reviews, 20(1), 133–163. doi:10.1128/cmr.00029-06.

[101] Silke Schelenz. (2008). Management of candidiasis in the intensive care unit, Journal of Antimicrobial Chemotherapy, 61, Issue suppl_1, pp. i31–i34, https://doi.org/10.1093/jac/dkm430.

[102] Gozalbo, D., Roig, P., Villamon, E., & Gil, M. (2004). Candida and Candidiasis: The Cell Wall as a Potential Molecular Target for Antifungal Therapy. Current Drug Target -Infectious Disorders, 4(2), 117–135. doi:10.2174/1568005043341046.

[103] Eggimann, P., Garbino, J., & Pittet, D. (2003). Epidemiology of Candida species infections in critically ill non-immunosuppressed patients. The Lancet Infectious Diseases, 3(11), 685–702. doi:10.1016/s1473-3099(03)00801-6.

[104] Douglas, L. J. (2003). Candida biofilms and their role in infection. Trends in Microbiology, 11(1), 30–36. doi:10.1016/s0966-842x(02)00002-1.

[105] Baillie, G. S., & Douglas, L. J. (1998). Effect of Growth Rate on Resistance ofCandida albicans Biofilms to Antifungal Agents. Antimicrobial Agents and Chemotherapy, 42(8), 1900–1905. doi:10.1128/aac.42.8.1900.

[106] Pathan Aslam R, Vadnere Gautam P, Singhai Abhay K, Kulkarni Bharti U. (2012). Peganum harmala: A Phyto-pharmacological Review. Inventi Rapid: Planta Activa, 2012(4):1-2.

[107] Bukhari N, Choi JH, Jeon CW, Park HW, Kim WH, Khan MA, Leet SH (2008). Phytochemical Studies of the Alkaloids from Peganum Harmala. Appl. Chem., 12(1): 101-104.

[108] Speziale, P., Pietrocola, G., Rindi, S., Provenzano, M., Provenza, G., Di Poto, A., Arciola, C. R. (2009). Structural and functional role ofStaphylococcus aureussurface components recognizing adhesive matrix molecules of the host. Future Microbiology, 4(10), 1337–1352. doi:10.2217/fmb.09.102.

[109] Isabela Araujo e Amariz, Jacyara Pereira da Silva, Emanuella Chiara Valença Pereira, Nathália Andrezza Carvalho de Souza, José Marcos Teixeira de Alencar Filho, Renan Nunes Pereira, Ana Paula de Oliveira and Larissa Araújo Rolim. (2019). Chemical study of Peganum harmala seeds, African Journal of Biotechnology, 18(21), pp. 462-471. DOI: 10.5897/AJB2019.16762.

[110] Sharaf, M., El-Ansari, M. A., Matlin, S. A., & Saleh, N. A. M. (1997). Four flavonoid glycosides from Peganum harmala. Phytochemistry, 44(3), 533–536. doi:10.1016/s0031-9422(96)00531-6.

[111] Darabpour, E., Poshtkouhian Bavi, A., Motamedi, H., & Seyyed Nejad, S. M. (2011). Antibacterial activity of different parts of Peganum harmala L. growing in Iran against multi-drug resistant bacteria. EXCLI journal, 10, 252–263.

[112] Pratama, M. R. F., Nasibova, T. A., Pratiwi, D., Kumar, P., & Garaev, E. A. (2020). Peganum harmala and its Alkaloids as Dopamine Receptor Antagonists: in Silico Study. DOI: 10.33263/BRIAC113.1030110316.

[113] Kumari JyotiMamta BaunthiyalAjeet Singh. (2016), Characterization of silver nanoparticlessynthesized usingUrtica dioicaLinn leaves andtheir synergistic effects with antibiotics, Journal of Radiation Research and Applied Sciences. https://www.sciencedirect.com/science/article/pii/S1687850715001132.

[114] Ezhumalai Parthibana, Nandhagopal Manivannan, Ravichandran Ramanibai & Narayanasamy Mathivanan. (2018). Green synthesis of silver-nanoparticles from Annona reticulata leaves aqueous extract and its mosquito larvicidal and anti-microbial activity on human pathogens, Biotechnology Reports, Vol. 21, https://www.sciencedirect.com/science/article/pii/S2215017X18302893.

[115] Robabeh Sabaghi Mianai, Mohammad Ali Ghasemzadeh & Mohammad Reza Zand Monfare. (2019), Green Fabrication of Cobalt NPs using Aqueous Extract of Antioxidant Rich Zingiber and

Their Catalytic Applications for the Synthesis of Pyrano[2,3-c]pyrazoles, Combinatorial Chemistry & High Throughput Screening. Vol. 22. Doi: 10.2174/1386207322666190307160354.

[116] Shahzadi, T., Zaib, M., Riaz, T. et al. (2019), Synthesis of Eco-friendly Cobalt Nanoparticles Using Celosia argentea Plant Extract and Their Efficacy Studies as Antioxidant, Antibacterial, Hemolytic and Catalytical Agent. Arab J Sci Eng, 44, 6435–6444. https://doi.org/10.1007/s13369-019-03937-0.

[117] M. Anandan, G. Poorani, P. Boomi, K. Varunkumar, K. Anand, A. Anil Chuturgoon, M. Saravanan, H. Gurumallesh Prabu. (2019). Green synthesis of anisotropic silver nanoparticles from the aqueous leaf extract of Dodonaea viscosa with their antibacterial and anticancer activities, Process Biochemistry, 80, pp. 80-88, ss. 1359-5113. https://doi.org/10.1016/j.procbio.2019.02.014.

[118] Shrivastava, S.; Dash, D. J. 2009. Nanotechnol. 2009, pp. 1–14.

[119] G. Sharmila, M. Thirumarimurugan. (2017). Phytofabrication, characterization and antibacterial activity of Cassia auriculata leaf extract derived CuO nanoparticles, J. Inorg. Organomet. Polym. Mater, 27, pp.668–673, https://doi.org/10.1007/s10904-017-0509-9.

[120] A Marzuki, V Suryanti, A Virgynia. (2017). Spectroscopic Study of Green Tea (Camellia sinensis) Leaves Extraction, IOP Conf. Series: Materials Science and Engineering, 193. Doi:10.1088/1757-899X/193/1/012049. https://iopscience.iop.org/article/10.1088/1757-899X/193/1/012049/pdf.

[121] G. Navarra, M. Moschetti, V. Guarrasi, M. R. Mangione, V. Militello, M. Leone. (2017). "Simultaneous Determination of Caffeine and Chlorogenic Acids in Green Coffee by UV/Vis Spectroscopy", Journal of Chemistry, vol. 2017, Article ID 6435086, 8 pages. https://doi.org/10.1155/2017/6435086.

[122] M.V. Mandke, S.-H. Han, H.M. Pathan. (2012), Growth of silver dendritic nanostructures via electrochemical route, Cryst. Eng. Comm. 14, pp. 86–89, https://doi.org/10.1039/C1CE05791J.

[123] S.Y. Lee, S. Krishnamurthy, C.-W. Cho, Y.-S. Yun. (2016). Biosynthesis of gold nanoparticles using Ocimum sanctum extracts by solvents with different polarity, ACS Sustain. Chem. Eng. 4, pp. 2651–2659, https://doi.org/10.1021/acssuschemeng. 6b00161.

[124] Stephan Link and Mostafa A. El-Sayed. (1999). Spectral Properties and Relaxation Dynamics of Surface Plasmon Electronic Oscillations in Gold and Silver Nanodots and Nanorods, J. Phys. Chem. B, Vol. 103, No. 40, pp.8410-8426. file:///C:/Users/Oscar/Desktop/Uv%20and%20nanoparticle.pdf.

[125] Yu, H., Chen, M., Rice, P. M., Wang, S. X., White, R. L. & Sun, S. (2005). Dumbbelllike bifunctional Au-Fe3O3 nanoparticles. Nano Letters, 5 (2), pp. 379–382.

[126] Macaluso, R. T. (2009). Introduction to Powder Diffraction and its Application to Nanoscale and Heterogeneous Materials. ACS Symposium Series, 75–86. doi:10.1021/bk-2009-1010.ch006..

CURRICULUM VITAE

Roshna ASHRAF ARIF

[redacted]

[redacted]

[redacted]